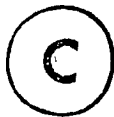


THE INFLUENCE OF TURBINE TIP
CLEARANCE ON THE FLOW IN A
RECTILINEAR WATER CASCADE

By
Nader Pezeshkzad

A thesis submitted to the Faculty of Graduate
Studies in partial fulfillment of the requirements
for the degree of Master of Engineering.



Department of Mechanical Engineering
McGill University
Montreal, Canada
December 1979

ACKNOWLEDGMENT

The author wishes to acknowledge the helpful cooperation of Drs. C. Murphy, A. Graham and U. Okapuu while conducting this research.

The efforts and cooperation of all of those who made the construction of the testing facilities possible is also appreciated.

ABSTRACT

An experimental investigation has been conducted to discover visually the flow mechanism in the rotor blade tip region for a particular turbine blade (R12). Flow visualization was obtained using tracer balls suspended in the fluid, and also with localized dye injection. The latter turned out to be more helpful.

The leakage mechanism present in the rotor blade tip region for a circumferentially grooved casing wall was investigated in detail. It was found that the leakage flow, and the "anti-leakage" flow, both directly depend on the pressure difference across the blade tip. The leak blockage mechanism works more efficiently at thicker parts of the blade. It was also found that the circumferentially grooved wall would be more advantageous for smaller tip clearances. A modified blade tip profile is proposed which would reduce tip clearance losses.

RESUME

Une recherche expérimentale a été entreprise en vue de découvrir de façon visuelle, le mécanisme du débit dans la région de l'extrémité de l'aube d'une turbine pour une aube particulière (R12). La visualisation du débit a été obtenue à l'aide de balles traçantes suspendues dans le fluide ainsi qu'à l'aide d'une injection localisée de colorant. Ce dernier procédé s'est révélé plus utile.

Une étude détaillée a été consacrée au mécanisme du coulage qui se produit dans la région en question pour un mur de revêtement à rainures circulaires. Elle a révélé que le débit du coulage ainsi que le débit "anti-coulage" dépendent tous deux directement de la différence de pression le long de l'extrémité de l'aube. Le mécanisme de blocage du coulage fonctionne de manière plus efficace dans les parties plus épaisses de l'aube. Il a été révélé également que le mur à rainures circulaires serait plus avantageux pour des intervalles plus petits des extrémités. Nous proposons un profil modifié de l'extrémité de l'aube, ce qui réduirait les pertes dues à l'intervalle entre l'extrémité et le mur de revêtement.

TABLE OF CONTENTS

	<u>PAGE NO.</u>
1. <u>INTRODUCTION</u>	1
1.1 Previous investigations	
1.2 Definition of the problem	
2. <u>DESCRIPTION OF THE RIG</u>	4
3. <u>FLOW VISUALIZATION</u>	6
3.1 Neutrally buoyant polystyrene balls	
3.2 Dye injector	
4. <u>OBSERVATIONS ON SMOOTH BELT USING TRACER BALLS</u>	8
4.1 The qualitative effect of tip clearance variation	
4.2 The qualitative effect of speed variation	
5. <u>OBSERVATIONS ON SMOOTH BELT USING DYE INJECTION TECHNIQUE</u>	11
5.1 Definition of Leakage line criterion	
5.2 Definition of Pressure side streamline direction criterion	
5.3 Definition of Blade tip clearance leakage direction criterion	
5.4 Definition of Vortex boundary criterion	
5.5 The quantitative effect of tip clearance variation	
6. <u>OBSERVATIONS ON GROOVED BELT USING DYE INJECTION TECHNIQUE</u>	15
7. <u>CONCLUSIONS</u>	18
8. <u>RECOMMENDATIONS FOR FUTURE RESEARCH</u>	20
9. <u>REFERENCES</u>	21

10. FIGURES

- Fig. 1: WATER FLOW ANALOGY RIG
- 2: R12 BLADE TIP CASCADE
 - 3: SCHEMATIC DIAGRAM OF BLADE R12 AND SECONDARY VORTICES
 - 4: WATER RIG WITH THE SMOOTH RUBBER BELT INSTALLED
 - 5: GROOVED BELT READY FOR INSTALLATION
 - 6: MERCURY VAPOUR LAMP
 - 7: DEFINITION OF VIEWING PLANES IN CASCADE CHANNEL
 - 8: VIEWING PLANES IN THE CASCADE TOP VIEW
 - 9: DYE INJECTOR
 - 10: CONTROL PANEL OF DYE INJECTOR
 - 11: PASSAGE VORTEX AT ZERO CLEARANCE
 - 12: TRAILING VORTICES AT ZERO CLEARANCE
 - 13: SUCTION SURFACE FLOW DISTRIBUTION AT ZERO CLEARANCE
 - 14: PRESSURE SURFACE FLOW DISTRIBUTION AT ZERO CLEARANCE
 - 15: EFFECT OF VARIATION OF TIP CLEARANCE
 - 16: EFFECT OF TIP CLEARANCE ON TRAILING VORTICES
 - 17: EFFECT OF SPEED VARIATION
 - 18: DEFINITION OF LEAKAGE LINE CRITERION
 - 19: DEFINITION OF PRESSURE SURFACE STREAMLINE DIRECTION,
TIP LEAKAGE FLOW DIRECTION, AND SECONDARY VORTICES
BOUNDARY CRITERIA
 - 20: OBSERVATION RESULTS FOR 2.5% CLEARANCE BETWEEN BLADE
R12 AND MOVING SMOOTH BELT
 - 21: OBSERVATION RESULTS FOR 2% CLEARANCE BETWEEN BLADE
R12 AND MOVING SMOOTH BELT
 - 22: OBSERVATION RESULTS FOR 1.5% CLEARANCE BETWEEN BLADE
R12 AND MOVING SMOOTH BELT

- 23: OBSERVATION RESULTS FOR 1% CLEARANCE BETWEEN BLADE R12 AND MOVING SMOOTH BELT
- 24: FLOW MECHANISM INSIDE THE GROOVES
- 25: FLOW MECHANISM ALONG THE GROOVES
- 26: THREE DIFFERENT TYPES OF LEAKAGE FLOW PATTERNS
- 27: OBSERVATION RESULTS FOR 2.5% CLEARANCE BETWEEN BLADE R12 AND STATIONARY GROOVED BELT
- 28: OBSERVATION RESULTS FOR 2% CLEARANCE BETWEEN BLADE R12 AND STATIONARY GROOVED BELT
- 29: OBSERVATION RESULTS FOR 1.5% CLEARANCE BETWEEN BLADE R12 AND STATIONARY GROOVED BELT
- 30: OBSERVATION RESULTS FOR 1% CLEARANCE BETWEEN BLADE R12 AND STATIONARY GROOVED BELT
- 31: OBSERVATION RESULTS FOR 2.5% CLEARANCE BETWEEN BLADE R12 AND MOVING GROOVED BELT
- 32: OBSERVATION RESULTS FOR 2% CLEARANCE BETWEEN BLADE R12 AND MOVING GROOVED BELT
- 33: OBSERVATION RESULTS FOR 1.5% CLEARANCE BETWEEN BLADE R12 AND MOVING GROOVED BELT
- 34: OBSERVATION RESULTS FOR 1% CLEARANCE BETWEEN BLADE R12 AND MOVING GROOVED BELT
- 35: RECOMMENDED BLADE TIP CONFIGURATION FOR REDUCTION OF THE LEAKAGE FLOW

1. INTRODUCTION

A small research turboshaft engine with a mass flow rate of 5.75 kg/s, and an output of 1500kw is being designed at Pratt & Whitney to operate at a cycle pressure ratio of 10:1 with a turbine inlet temperature of 1350k. This high compression ratio together with small mass flow results in a turbine design with a small annulus area, and a small blade height (2.88cm). High potential gas flows through small turbine blades increases the percentage losses due to tip clearance. To help reduce these losses, an understanding of the tip flow associated with varying the radial clearance and shroud geometry is required.

The main objective of this thesis is to study experimentally the flow characteristics at the blade tip region for different tip and shroud geometries. An understanding of the flow mechanisms in this region will lead to better geometries in order to reduce the tip clearance losses. This investigation consists of making visual observations in order to discover the flow mechanisms present in the blade tip and shroud region.

1.1 Previous investigations

Over the past 60 years, several investigations have been conducted to determine the rotor tip clearance penalty for various turbine designs.

So far, the theoretical studies which have been conducted on this subject involve many assumptions which limit the practicality of the results and thus can only be used to serve as guidelines. When a new blade tip geometry, or casing wall configuration is used; the only sure way of achieving optimum tip clearance for that particular turbine is to experimentally vary the tip clearance under actual operating conditions, while measuring the most appropriate indicator of performance for that particular turbine

application.

An almost universal parameter in this subject is the "efficiency gradient". This is the percentage loss of efficiency for a change of one percent of the blade height at a given clearance. This correlation has little theoretical involvement with the physics of the situation, as it is obtained from experimental data taken for a particular type of turbine. However, use of the efficiency gradient is valid for relatively similar conditions; bearing in mind that some factors do not affect the tip clearance losses (e.g., the blade height), and others do (e.g., the pressure ratio).

The interesting point is that despite the different experimental techniques, the investigators have arrived at similar values for the efficiency gradient. For example, Hass & Kofsky (Ref. 1) and Rylatt & Patel (Ref. 2) have reported a 2% efficiency loss for a 1% tip clearance increase. This tip clearance ratio is based on the blade height. Some investigators referring to the nonlinear behavior of the efficiency gradient have reported a range of efficiency drops. For example, Hebbel (see Ref. 2) reported a 1.5 to 2% efficiency drop, in a similar way Okapuu (see Ref. 2) reported a 2.0 to 2.5% fall in stage efficiency for a 1% blade height increase in clearance.

Among all of the previous investigations the one that is most applicable to the present study, is the recent investigation of Hass and Kofsky on the effect of recessed casing configuration on overall performance of a small axial-flow turbine (Ref. 1).

Using a recessed casing configuration, Hass and Kofsky's research shows a 0.5% efficiency gain for a 1% tip clearance decrease. Test results on the Pratt & Whitney turbine, having a circumferentially grooved casing wall configuration, show a 0.5% efficiency gain for a 1% tip clearance

decrease. The tests were carried out for a 1% tip clearance only.

1.2 Definition of the problem

The importance of tip clearance losses in small jet engines has attracted the attention of jet engine manufacturers. They are supporting research programs to find an appropriate casing wall configuration to reduce tip clearance losses.

In 1976 at Pratt & Whitney three different casing wall configurations were tested for two types of blade designs. It was found that a circumferentially grooved casing wall reduced the tip leakage for R12 blades, while the tip leakage for another type of blade (PT6 Hp turbine blade) was increased compared to a plane casing wall condition. In order to understand why there was a difference, it was decided to study the flow visually in a dynamically simulated rectilinear water cascade tunnel with a belted moving surface to simulate the relative motion between the blades and the shroud.

This work was started in 1977 by designing an appropriate water-flow analogy testing facility. This was designed for a wide variety of studies. Its construction was completed in 1978. Visual observations were started in September 1978 and finished in November 1979.

2. DESCRIPTION OF THE RIG

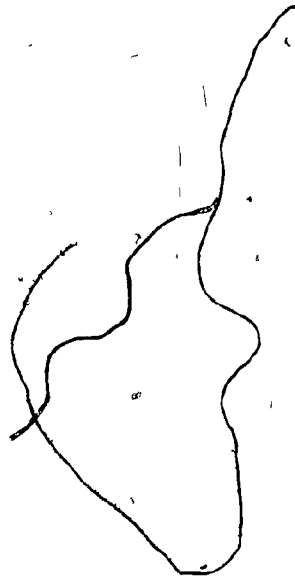
As far as flow visualization is concerned, the use of a water flow analogy test rig is essential. Velocities of the order of 18000cm/sec related to the prototype gas turbine, can be scaled down to the order of 15cm/sec in a water cascade with a geometric model to prototype scale factor of 8:1 and maintain dynamic similarity.

The water flow analogy rig (Fig. 1) utilizes a recirculating water system. Water is pumped from a storage tank (lower right) into a header tank (upper left), from which it flows through the test section (upper right) and returns to the storage tank. The maximum water flow is 6.75 litre/sec delivered at a maximum head of 6.1m.

Fig. 2 shows the blade cascade installed in the working area. In practice a wide variety of internal flow models could be installed. The cascade consists of five plexiglass blades, each 16.51cm long, having a constant cross section modelled on the R12 blade tip cross section (Fig. 3). The blades hang vertically with the simulated tip clearance at the floor of the cascade. The tip clearance separation is controlled by vertical adjustment of the location of the blade cascade. The cascade duct and the blades are made of transparent plexiglass. Across the cascade floor beneath the blades, runs a belt which simulates the relative motion of the blade with respect to the shroud. The solid casing wall of the engine is modelled by a smooth rubber belt (Fig. 4). This is driven by a variable speed compressed air motor. A grooved belt simulates the circumferentially grooved casing wall of the engine. The grooved belt consists of a number of aluminum elements which are pinned to a rubber belt (Fig. 5).

The scale of the model is eight times larger than the prototype,

at the tip section. The duct is run full of water in order that the flow in the blade channels would have solid borders, and thus could also have secondary flows in the correct location. With full flow, this gives a reasonable simulation of the engine Reynolds number, thus ensuring dynamic similarity. Compressibility effects are not modelled. This and the partial simulation caused by the Rectilinearity of the water cascade constitute the main limitations of the test rig.



3. FLOW VISUALIZATION

A means of observing actual streamlines is of great value when analyzing flow characteristics. Frequently when the flow is complicated direct measurements are difficult to interpret and flow visualization is the best technique to use.

In order to visualize streamlines a visible substance must be introduced into the flow so that they follow the streamlines closely without changing the flow pattern appreciably. Two kinds of visible substances were used to analyze the flow patterns: neutrally buoyant particles and tracer fluid or dye.

3.1 Neutrally buoyant polystyrene balls

In this method, neutrally buoyant polystyrene balls of approximately 0.5mm diameter are mixed with water in the storage tank. As they travel with the water flow they pass through 6 screens along the water channel which help to make the flow laminar and evenly distribute the balls. As the water flow becomes laminar the tracer balls move along the streamlines so that when the water flow passes through the blade passage, and the tip clearance, they follow the flow patterns developed.

A planar beam from a mercury vapour lamp was used to illuminate the tracer balls as they move along the flow streamlines (Fig. 6).

To investigate the characteristics of the secondary vortices and tip clearance leakage flow, ten observation planes were chosen. The planar beam would illuminate the tracer particles which pass through these viewing planes (Figs. 7, 8).

Flow streamlines are not generally located on the planes of

illumination and only a short segment of a streamline can be pursued at one time using tracer balls. Therefore this method was used only for preliminary experiments on the general characteristics of the flow inside the blade passage. Although this method is easily applied for macroscopic observation; for microscopic observation of the flow, a versatile dye injector was used.

3.2 Dye injector

This technique consists of injecting a dye into the flow at any arbitrary point inside the blade passage. The dye will follow the local streamlines, which can thus be visualized (Fig. 9).

The location of the tube head can be varied to overcome the problem of rapid dispersion of the dye in the water. Even minor eddies can be discovered with dye injection by moving the injector tube head close to the region of study. The tube head is controlled through three knobs and a small winch wheel outside of the water tunnel (fig. 10).

The use of these flow visualization techniques made possible the discovery of some unknown three-dimensional flows in the tip region, which provided the essential experimental information for this investigation.

In spite of the difficulties in getting quantitative experimental data on flow quantities, the visualization techniques provided a good approximation for these quantities from the geometry of the streamlines.

4. OBSERVATIONS ON SMOOTH BELT USING TRACER BALLS

A set of observations was made by illuminating tracer balls, to investigate the general characteristics of the main flow.* The clearance space was changed from 0 to 2% of the blade height. The smooth belt was operated at two speeds; one, a tip to shroud relative speed to match the Reynolds number at the prototype design speed; and two, three times as fast. Observations were also taken with the belt stationary. The characteristics of the secondary vortices changed as the tip clearance separation and the wall relative velocity changed.

When the wall relative velocity was zero, and the blade tip touched the wall (zero clearance), the only sizeable vortex present inside the blade channel was the passage vortex. The passage vortex forms in the root and tip corners of the blade channel due to the turning of the flow.

Fig. 11 shows the evidence of the passage vortex in the observation planes 2, 3, 4. Plane 1 shows there is a relatively small stall region in the entering flow at the corner of the pressure side and the stationary belt. This decrease in velocity at the leading edge, as will be discussed later, is a function of the tip clearance. In other words, when the tip is close to the belt, the stagnation line moves away from the leading edge towards the trailing edge. Plane 3 shows the passage vortex starting to roll up in the suction side corners. Plane 4 shows the passage vortex developed.

Fig. 12 depicts the formation of trailing vortices. These are caused by different flow distributions in the pressure and suction sides of the blade downstream from the trailing edge. Plane 5 (Fig. 12) shows how the flow

* It was not possible to photograph the illuminated balls. The flow patterns were carefully observed and the explanatory figures were drawn.

near the pressure side slowly moves down toward the trailing edge, and also depicts the position of the passage vortex on the suction side leaving the blade. Plane 6 shows the formation of Von Karman eddies, which move downstream as observed in planes 7 and 8. This disturbance to the channel flow caused by the trailing edge vortices is one of the sources of loss of the fluid energy. Fig. 13 depicts the suction surface flow. The convergence which is very marked in the upper and lower parts of the flow is due to the passage vortex in the blade channel. Fig. 14 shows the streamlines adjacent to the pressure surface. Here the divergence due to the passage vortex is seen.

4.1 The qualitative effect of tip clearance variation

At zero belt speed, the tip clearance was changed and observations were taken for the; zero tip clearance, 0.5% tip clearance, and 2% tip clearance. Fig. 15 shows the effect of varying the tip clearance separation on the characteristics of the blade passage flow at the tip region.* Fig. 15a corresponds to zero clearance and zero belt speed, where only the passage vortex is present.

As the tip clearance increases, fluid starts to flow from the pressure side to the suction side. At the small 0.5% clearance, leakage flow is not able to form a vortex, and the location of the passage vortex remains almost the same as that for zero clearance (Fig. 15b).

* Flow characteristics at the root region of the blade passage was almost independent of the clearance and belt motion, and remained unchanged (the same as the zero clearance situation). So, for convenience of comparison, only the tip region is shown in the Figures.

At a tip clearance equal to 2% of the blade height, a strong clearance vortex occupies the tip corner of the suction side and the passage vortex is markedly modified as a result of the presence of the tip clearance vortex. Plane 4 (Fig. 15c) shows the location of the passage vortex that has moved from the suction side corner to the pressure side corner.

Fig. 16 shows that for the 2% clearance, trailing vortices transform to a downward flow which is the result of the clearance vortex being in accordance with the passage vortex.

4.2 The qualitative effect of speed variation

When the belt is moving, a wall boundary layer exists which influences the tip leakage flow. Here the effect of speed variation for the 2% clearance separation is discussed.

Fig. 17a, represents secondary flows corresponding to the stationary belt condition. Fig. 17b shows the reinforcement of the passage vortex as a result of combining with the scraping vortex, which is caused by the motion of the belt. The wall boundary layer occupies a portion of the tip clearance. So, the tip leakage flow is reduced. As a result of this leakage flow reduction, and the existence of the combined passage and scraping vortices, the tip clearance vortex gets weaker.

When the belt speed is three times as fast at the equivalent of the tip to shroud relative velocity of the prototype turbine at the design point (Fig. 17c), the belt surface boundary layer causes more resistance against the clearance leakage. In this condition the wall boundary layer thickness increases, which reduces the clearance leakage, but reinforces the strength of the combined passage and scraping vortices.

5. OBSERVATIONS ON SMOOTH BELT, USING DYE INJECTION TECHNIQUE

A set of observations was made by using dye as a tracer fluid to investigate the small scale characteristics of the tip clearance flow. The clearance space was changed from 1% to 2.5% of the blade height and the smooth belt was operated at a speed equivalent to a tip to shroud relative velocity of the prototype turbine at the design point.

The criteria used for this set of observations are as follows:

5.1 Leakage line

The leakage line is defined as the locus of the points where the streamlines start to turn toward the pressure side and pass under the tip. It is located at the blade tip level. The location of this line depends on the clearance leakage flow rate. At the zero tip clearance, the leakage line will lay along the pressure side corner with the belt surface. As the clearance leakage rate increases, the leakage line moves farther away from the blade pressure side. Fig. 18 shows the "leakage horn" which consists of that portion of the blade channel flow that passes through the clearance gap from the pressure side to the suction side of the blade. The leakage line is the intersection of the "leakage horn" and an imaginary plane at the blade tip level.

5.2 Pressure side streamline direction

The direction of the streamlines adjacent to the pressure surface of the blade depends on the rate of the clearance leakage flow.

At the zero leakage flow the streamlines have the same direction as the streamlines of the zero tip clearance situation (Fig. 14). As the

leakage flow rate increases, the angle between the streamlines and the blade tip increases (Fig. 19).

5.3 Blade tip clearance leakage direction

The direction of the tip clearance leakage flow, depends on the pressure distribution on both sides of the blade, the belt surface boundary layer, and finally the blade tip boundary layer. At relatively small clearance separations, the belt surface boundary layer creates a resistance against the pressure driven leakage flow and reduces the tip clearance leakage flow. This leakage reduction affects the direction in which fluid particles take to go from the pressure side to the suction side.

As the leakage flow rate is reduced, flow patterns over the tip turn towards the trailing edge (Fig. 19).

5.4 Vortex boundary

Since the loss of the fluid energy depends on the intensity of turbulence, an approximate boundary of the vortices present in the channel indicates the rate of main flow disturbances caused by the clearance vortex and combined passage-scraping vortex (Fig. 19).

5.5 THE QUANTITATIVE EFFECT OF TIP CLEARANCE VARIATION FROM DYE INJECTION

At the equivalent design point speed, tip clearances were changed and the observations were taken at 1%, 1.5%, 2%, and 2.5% of the blade height.

Each set of observation planes consists of: the top view, front view, and a cross section along the blade in the proximity of the maximum leakage area (Fig. 20). The top view in each observation plane set shows the location of the leakage line, clearance leakage streamlines, tip clearance vortex, and combined passage-scraping vortex. The front view depicts the pressure side streamline direction. The cross section view shows the mechanism of tip leakage and wall boundary layer roll-up.

Fig. 20 shows a set of observation planes for 2.5% tip clearance. The top view represents the blade tip area, looking downwards from above. The direction of the flow through the clearance gap is shown.

The first 25% of the axial chord length from the leading edge, at the top view of Fig. 20, has clearance velocities that are lower than the mid-chord section (as evidenced by the shorter vectors). It should be noted that the vortex does not start at the leading edge of the blade, but in this case, about one third of the way along the suction surface. This happens because the pressure gradients are weaker near the leading edge. Furthermore, for such a relatively large tip clearance separation, there is a greater unguided throughflow over the blade tip which follows the direction of the main flow, and passes through the tip and belt boundary layer with little mixing. So the leakage starts to roll up after the first third of the way along the suction surface.

Fig. 20 also shows the position of the leakage line, the vortices

boundary, and the direction of the pressure side streamlines. At the right side of Fig. 20 in the cross section view of the blade; the blade tip boundary layer, the belt surface boundary layer, and the mechanism of the leakage blockage through the belt surface boundary layer roll-up are recorded.

Fig. 21 represents the tip leakage mechanism for the 2% tip clearance condition. The major difference between the 2% and 2.5% tip clearance is the change in the position of the leakage line which depicts less unguided through flow over the blade tip. As a result, the leakage flow in the leading edge is mainly influenced by the pressure gradient. Slight changes are seen in the tip leakage directions and tip clearance vortex, predicting less tip leakage flow.

Fig. 22 represents the tip leakage mechanism for the 1.5% tip clearance condition. Comparing the leakage lines, tip leakage vortex, pressure streamline directions, and the blade cross section view between 1.5% and 2% tip clearance indicates only a slight reduction in the tip leakage flow.

Fig. 23 shows a sudden change from 1.5% to 1% tip clearance separation, especially the tip clearance vortex boundary and combined passage-scraping vortex have changed considerably (see top view). Another considerable change is noticed in the direction of the pressure surface streamline direction at the leading edge (see front view). This suggests reconsidering the blade profile design at the blade tip for a 1% tip clearance.

For purposes of leakage control, it can be noted that the leakage flow, for tip clearances above 2% of the blade height, is partly influenced by the unguided throughflow over the blade tip, and leakage reduction devices are needed all along the blade chord. Below 2% tip clearance, leakage flow is weak for the first 25% of the axial chord from the leading edge, and the last 25% of the axial chord to the trailing edge.

6. OBSERVATIONS ON THE GROOVED BELT USING DYE INJECTION TECHNIQUE

A set of observations were taken using dye to investigate the microscopic characteristics of the tip clearance flow present when a grooved belt was used in place of the flat belt.

The clearance separation was changed from 1% to 2.5% of the blade height. Initially, observations were taken within the stationary grooved belt, then observations of the flow patterns were taken with the grooved belt moving at a speed equivalent to a tip to shroud relative velocity of the prototype turbine at design point.

The mechanism of the leak blockage present in the blade tip region, which was discovered during the preliminary observations is as follows.

In each groove there are two circulating cells, one in the bottom of the groove and the other adjacent to the blade passage flow (Fig. 24). Along each groove, three different regions are distinguished (Fig. 25). Region A is characterized by a flow that enters into the groove and moves along the direction of the moving belt; next region B is characterized by a flow that enters the groove but moves to the opposite direction, and finally region C the efflux region for outgoing flow from the groove. In region C, which covers all of the blade tip surface, the two previous entering flows return to the blade passage flow, and block the tip clearance gap. Fig. 24 shows that the peak outflow in region C corresponds to the blade suction side. Fig. 24 also shows the blade tip boundary layer. The details of the flow characteristic inside the blade tip boundary layer is shown in Fig. 26.

There are three different types of leakage flow patterns. Pattern no. 1 (Fig. 26), represents the fast moving leakage flow streamline. Pattern

no. 2 represents the leakage flow streamline which is associated with the boundary layer of the groove outflow across the blade. Pattern no. 3 represents the slow moving leakage flow streamline.

Figure 27 shows a top view of the blade cascade (looking downwards from above through the transparent plexiglass blade), a front view of the blade, and a cross sectional view from the maximum leakage region (looking downstream). This was for; 2.5% tip clearance, and a stationary grooved belt condition.

The cross sectional view of the blade passage shows that flow near the belt enters into the groove from region A and B, and then near the suction side (region C) it flows out and blocks the leakage flow exit.

The leakage line configuration (top view) shows the absence of the wall boundary layer resistance to the unguided throughflow over the blade tip. So at the leading edge region, leakage is mainly supplied by the main flow and is not primarily under the control of a pressure gradient. The clearance vortex and combined passage-groove outflow vortex form on the suction side of the blade as indicated in the cross-section view.

Comparison between the different characteristics of the leakage flow mechanism for different clearances of 2.5%, 2%, 1.5%, and 1% for the stationary grooved belt condition shows very little improvement in the rate of the leakage flow (Figs. 27-30). This indicates that the wall boundary layer plays the main role in decreasing the leakage flow. This will be discussed further in the following paragraphs.

Fig. 31 corresponds to the observations in the 2.5% tip clearance with the grooved belt moving at the equivalent speed of the tip-shroud relative velocity in the prototype turbine at design point.

By comparing Figs. 27 and 31, a significant reduction in the tip leakage will be noticed. This sudden change which can only be attributed to the belt motion shows the important relation of the grooved belt speed and leakage flow reduction. In fact, the motion of the grooved belt has caused the groove outflow region to move further into the clearance gap and as a result clearance leakage has been reduced to less than the stationary grooved belt condition. This comparison indicates that: the leakage line has moved closer to the pressure side, the vortices occupy less space inside the channel, and the leakage flow directions have turned towards the trailing edge. Overall less leakage is obtained with the grooved belt moving than when it is stationary.

At the design point speed, by going from 2.5% to 2% tip clearance (Fig. 32) the leakage is reduced slightly. However, as the tip clearance is reduced to 1.5%, observation shows (Fig. 33) a considerable decrease in the rate of the leakage flow. At 1% tip clearance (Fig. 34) there is almost no leakage flow in the first half of the blade chord, and in the last 25% of the blade chord to the trailing edge. For the grooved belt condition the same profile defect is observed which suggests a reconsideration of the blade tip profile design of the leading edge (for 1% tip clearance).

7. CONCLUSIONS

7.1 Smooth belt

The observation results show that the rate of tip leakage flow is based on two factors; the pressure difference across the blade tip, and the casing wall boundary layer effect which opposes the pressure driven flow. Since the pressure difference across the blade tip for different tip clearances remains almost constant, the rate of leakage flow for a particular blade will be a direct function of interference of the casing wall boundary layer with the pressure driven flow boundary layer. This means that aside from the effect of pressure difference on the rate of leakage flow, any factor that causes more interference of these two boundary layers, such as tip clearance reduction, and increase of casing wall relative speed, will reduce the rate of tip leakage.

7.2 Grooved belt

The leakage mechanism present in the grooved belt condition indicates that the groove outflow blocks the way for the pressure driven leakage flow. The interesting point is that the leakage flow and "anti-leakage" flow both directly depend on the pressure difference across the blade tip. So, for thick parts of the blade where pressure driven leakage flow is sizeable, the blockage mechanism works more efficiently. The blade tip thickness also exerts some influence on the pressure driven leakage flow. In fact, groove outflow beneath the blade tip at thick parts of the blade makes a wider interference zone with the pressure driven leakage flow boundary layer on the blade tip. Therefore, the circumferentially grooved casing wall configuration is more appropriate for blades with thicker tip profiles. This phenomenon can be better observed by comparison of the results

for both the smooth belt and the grooved belt conditions. This indicates that around the trailing edge, where the blade tip profile is thinner, the leakage streamline directions are unchanged.

Comparing Figs. 20, 21, 22, and 23 with 31, 32, 33, and 34 respectively, indicates that a circumferentially grooved wall will be more advantageous for smaller tip clearances. This effect is most evident from the deflection of the direction of the clearance leakage flow streamline towards the trailing edge. Another outcome of the comparison of the leakage mechanism between the solid casing and the circumferentially grooved casing wall configuration is that the leakage line for the latter one is generally closer to the pressure surface for similar running conditions (tip clearance and rotational speed). Therefore a smaller mini-shroud blade* would be sufficient for a certain amount of leakage reduction on the solid casing configuration.

* A blade with partial shroud seal at the tip.

8. RECOMMENDATIONS FOR FUTURE RESEARCH

For visualization techniques more accurate results would be expected using an electronic particle position indicator.

For tip clearances of 1% of the blade height, it was found that a portion of the pressure side flow near the tip at the leading edge turns back and moves towards the suction surface (Figs. 23 and 34). It is recommended that the blade tip profile at the leading edge should be reconsidered to reduce leakage losses for tip clearances less than 1%.

It appears that some of tip leakage flow can be prevented by altering the blade tip configuration. A blade tip configuration is suggested by the author as shown in Fig. 35. The blade tip profile at the pressure side edge is extended to the leakage line to reduce unguided leakage flow. The blade tip at the suction side edge is curved to reduce the intensity of the tip clearance vortex.

9. REFERENCES

1. Haas, J.E. and Kofskey, M.G. "Effect of Rottor tip clearance and configuration on overall performance of a 12.77 Centimeter Tip Diameter Axial-Flow Turbine" ASME 79-GT-42, 1979.
2. Graham, J.A.H. "Literature Survey on Tip Clearance Losses in Turbines", 1978.
3. Rains, Dean, A. "Tip Clearance Flows in Axial Flow Compressors and Pumps", 1954.

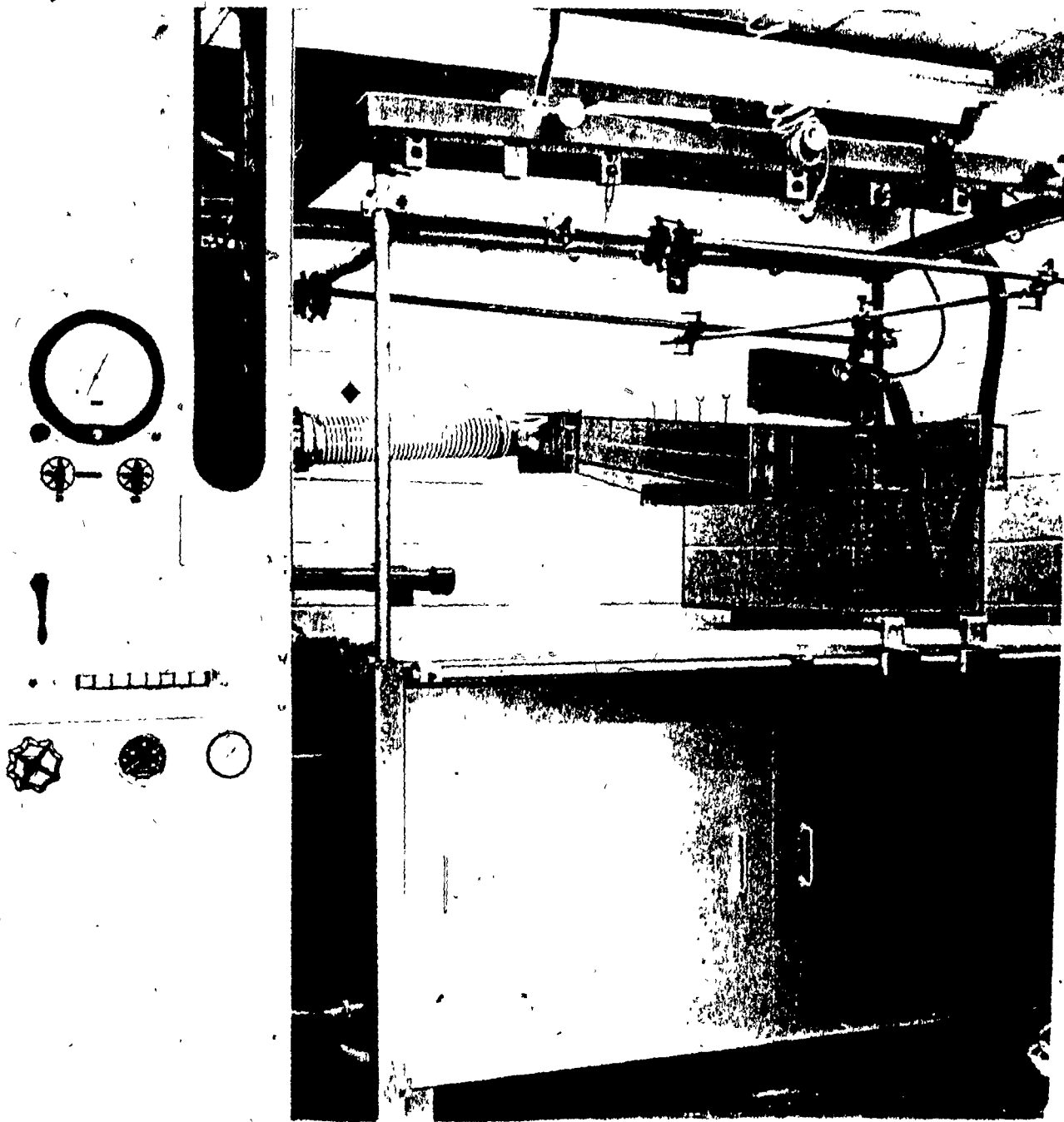


Fig. 1: WATER ANALOGY RIG

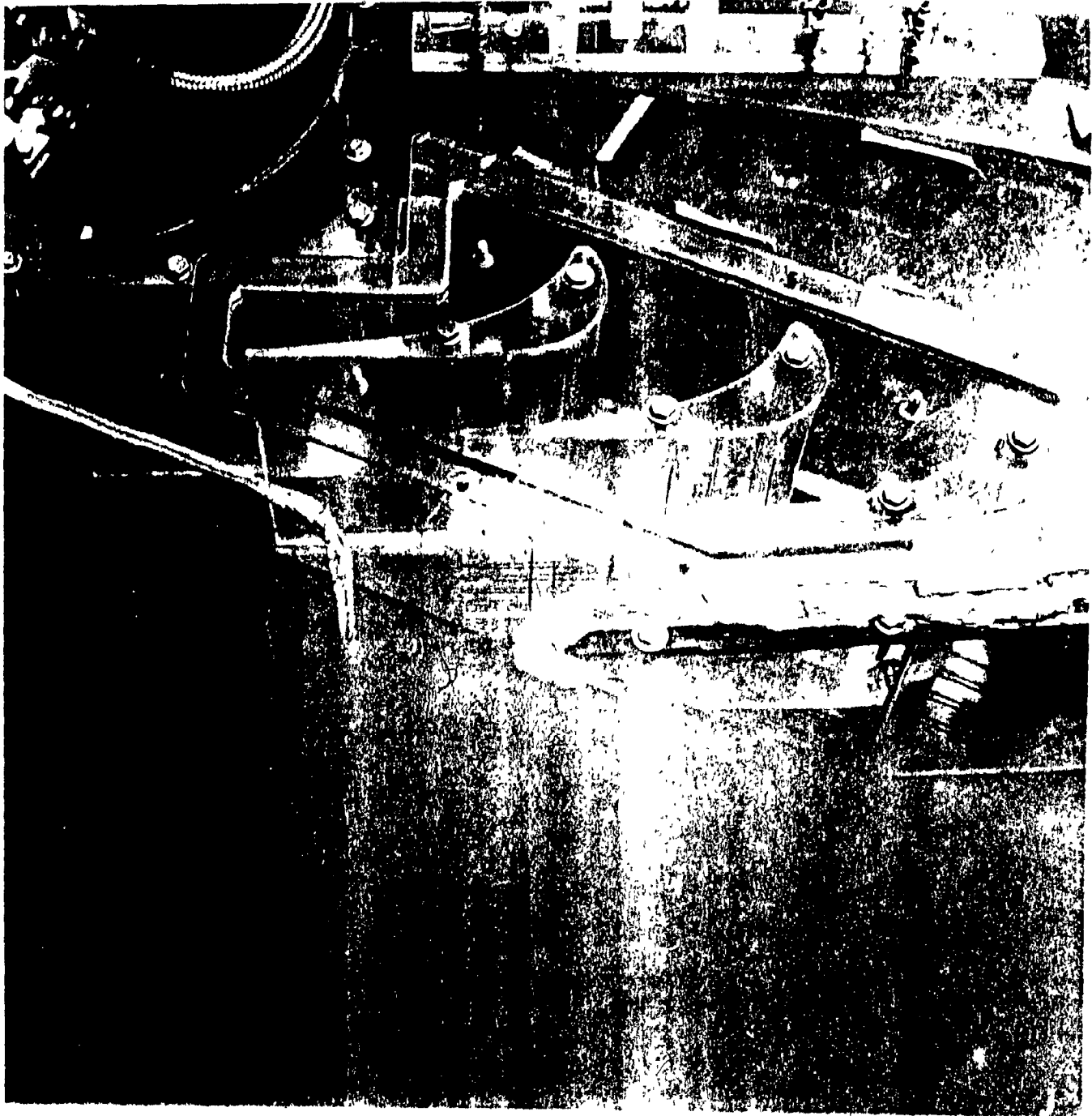


Fig. 2: R12 BLADE TIP CASCADE

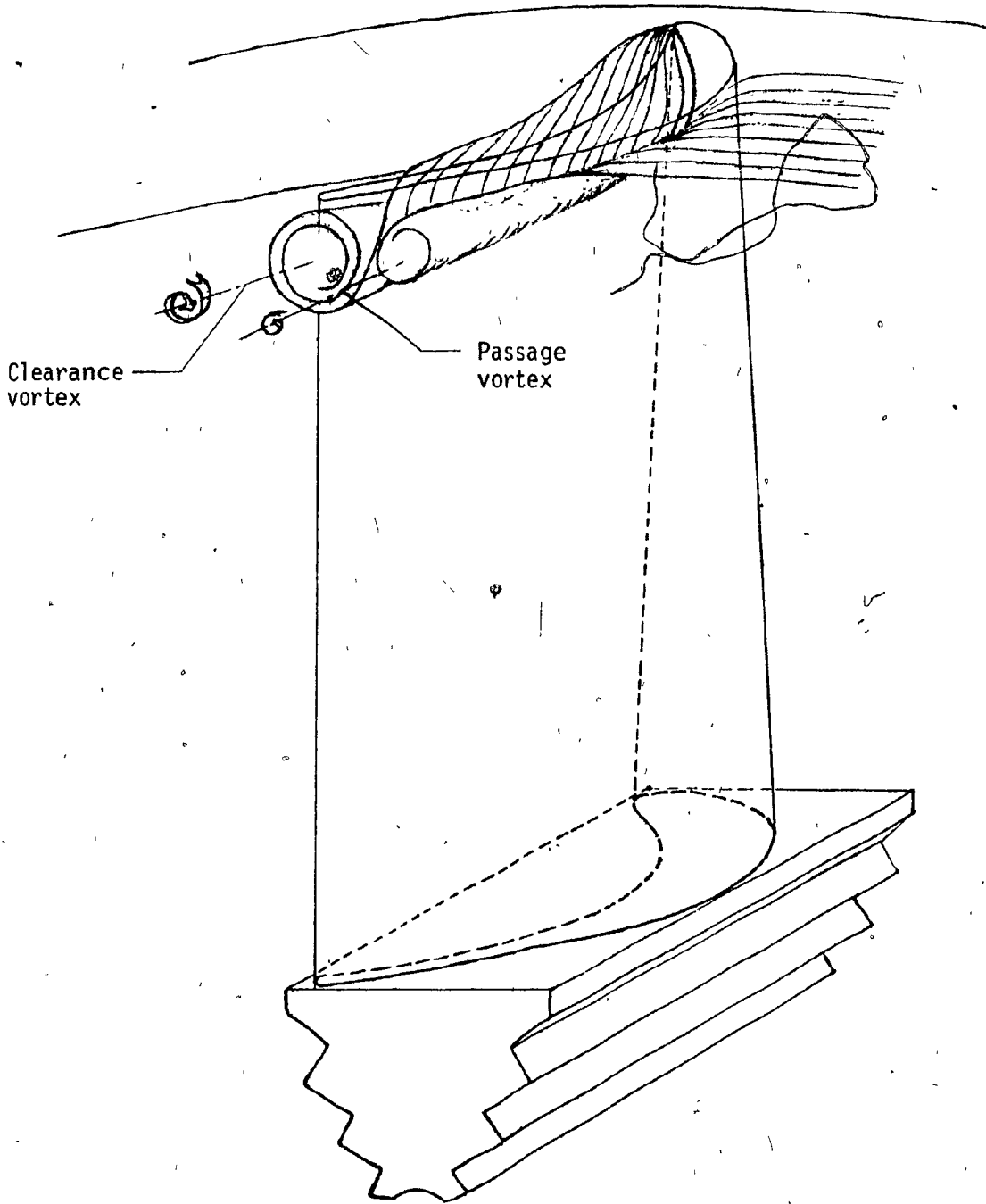


Fig. 3: BLADE R12, SECONDARY VORTICES AND THEIR DIRECTION.

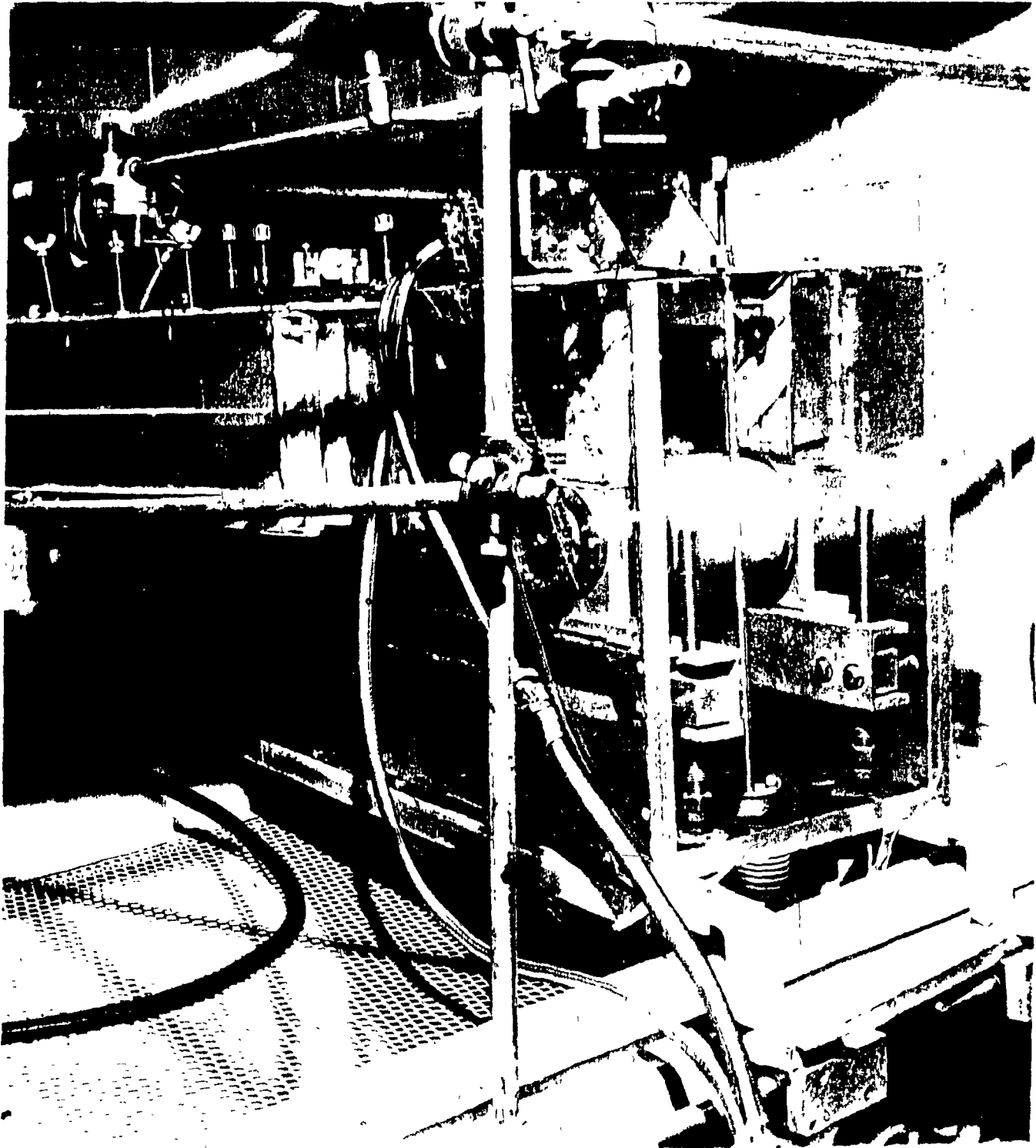


Fig. 4: WATER RIG WITH THE SMOOTH RUBBER BELT
INSTALLED.

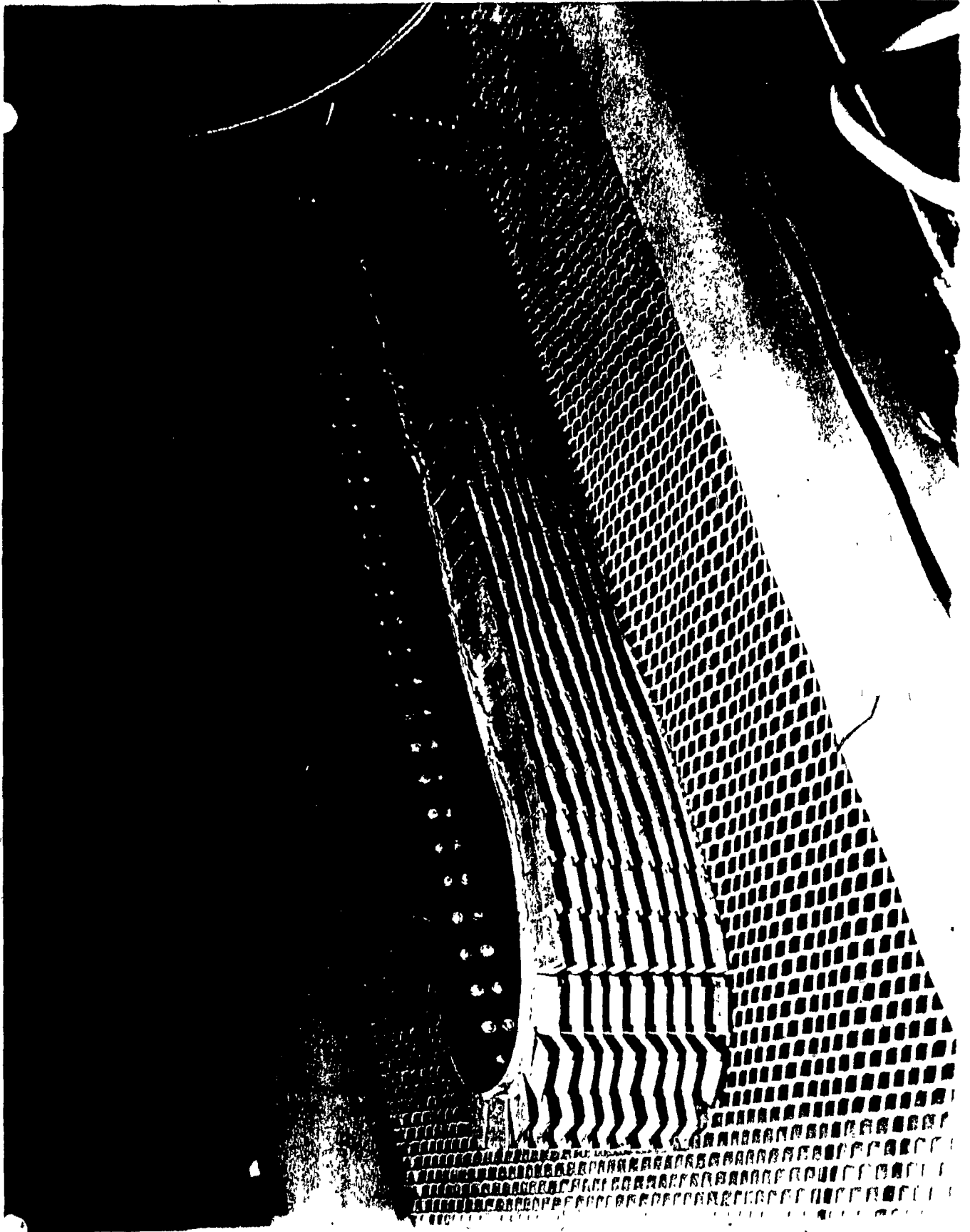


Fig. 5: THE GROOVED BELT READY FOR INSTALLATION.

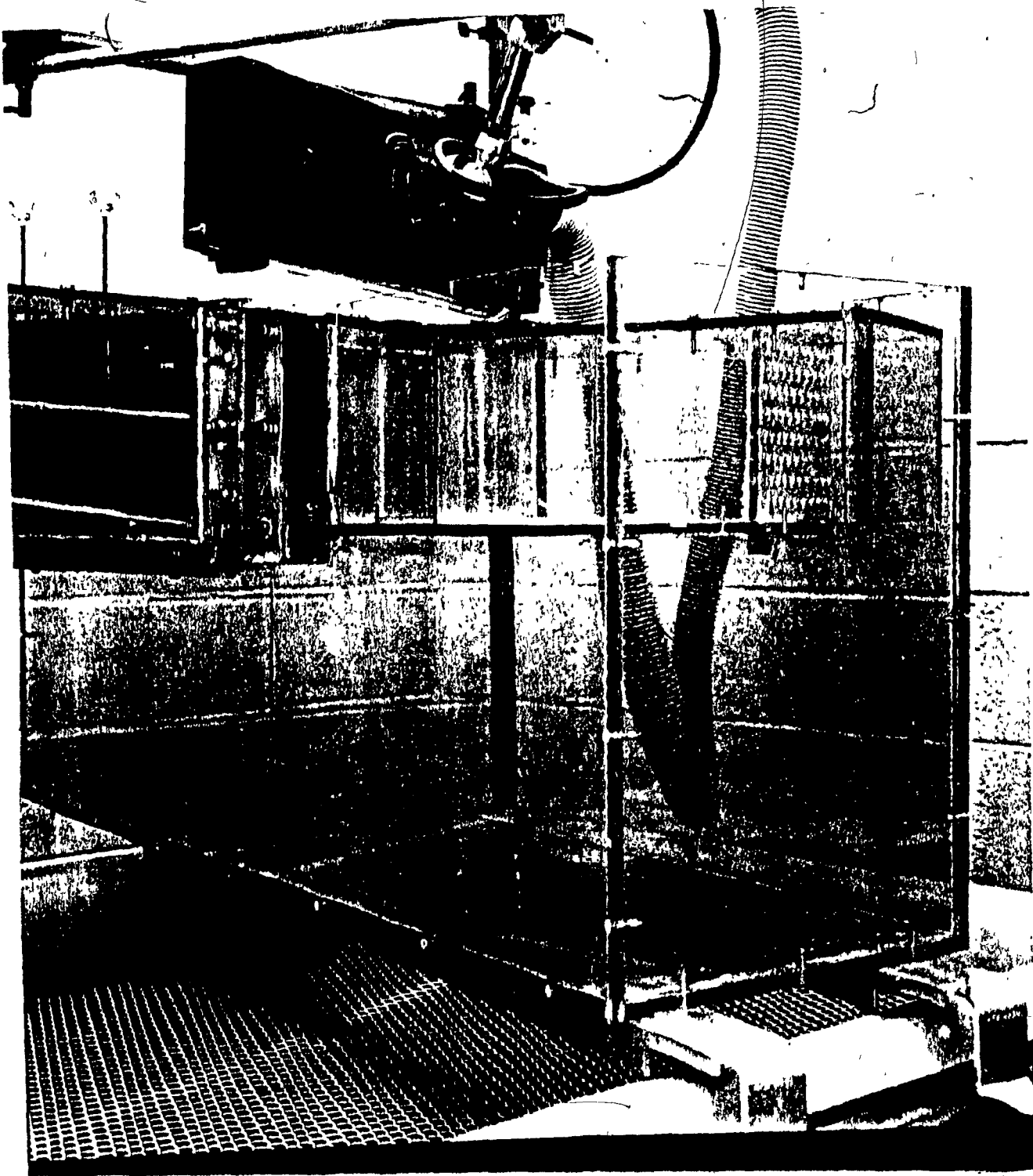


Fig. 6: MERCURY VAPOUR LAMP.

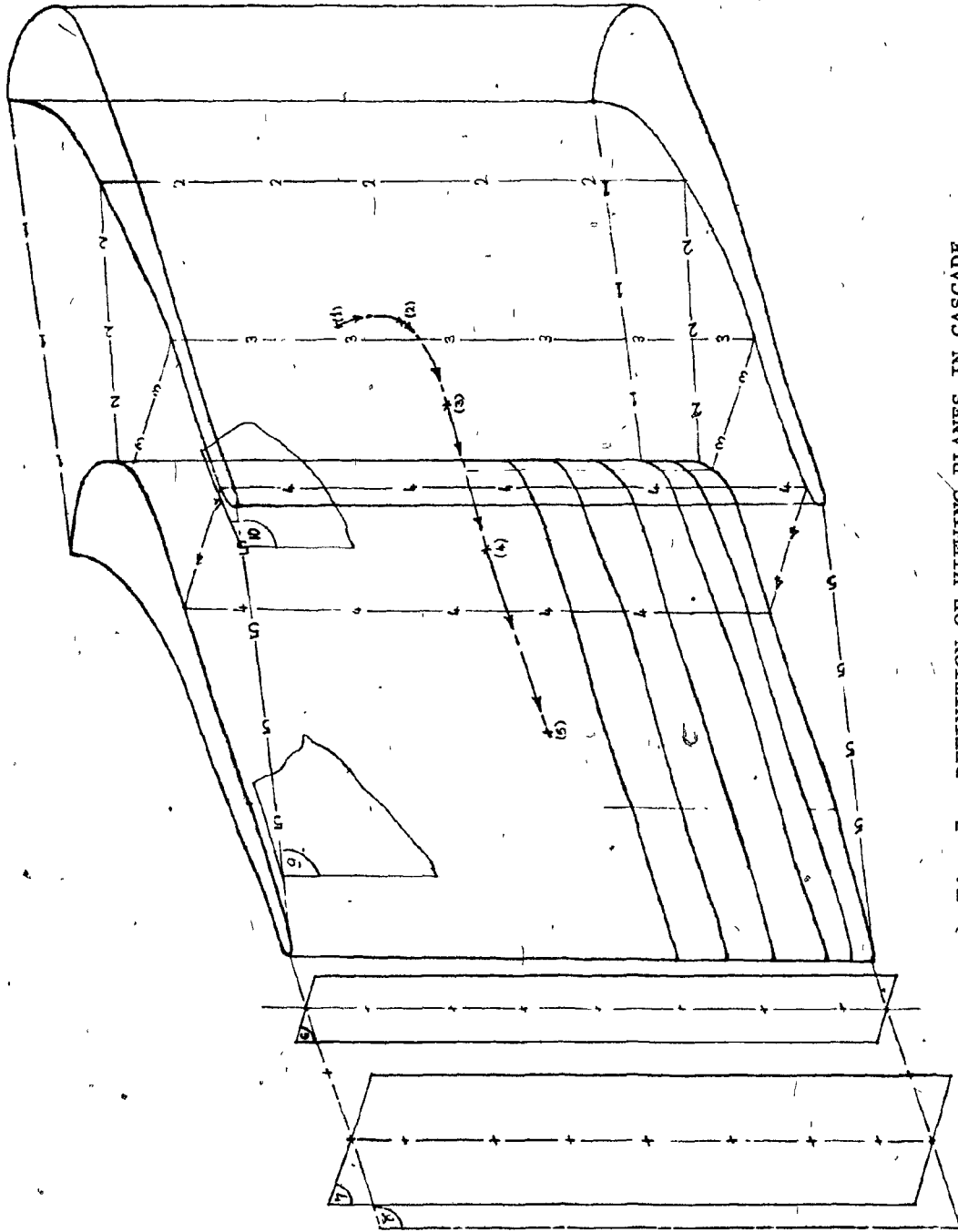


Fig. 7: DEFINITION OF VIEWING PLANES IN CASCADE

CHANNEL.

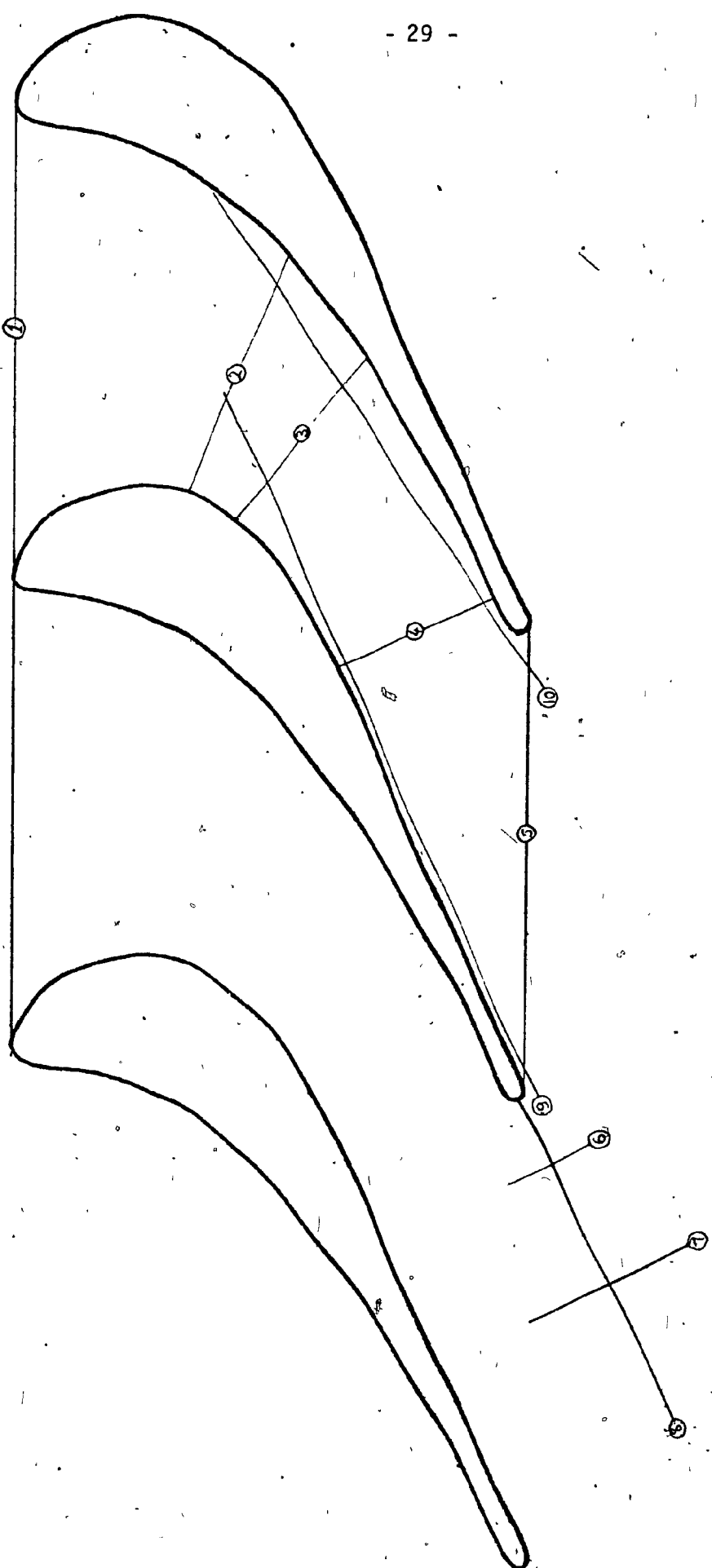


Fig. 8: VIEWING PLANES IN THE CASCADE TOP VIEW.

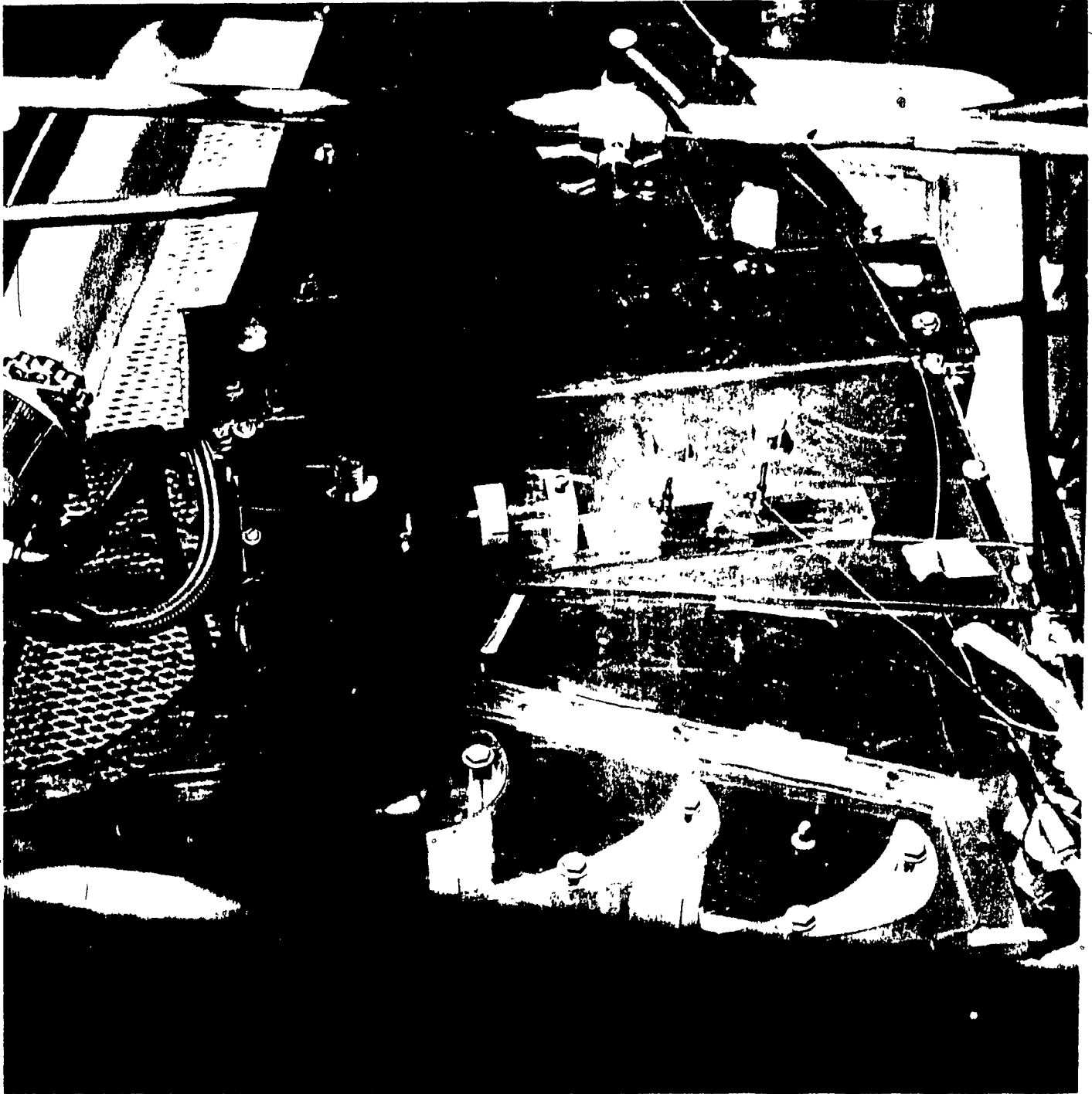


Fig. 9: DYE INJECTOR.

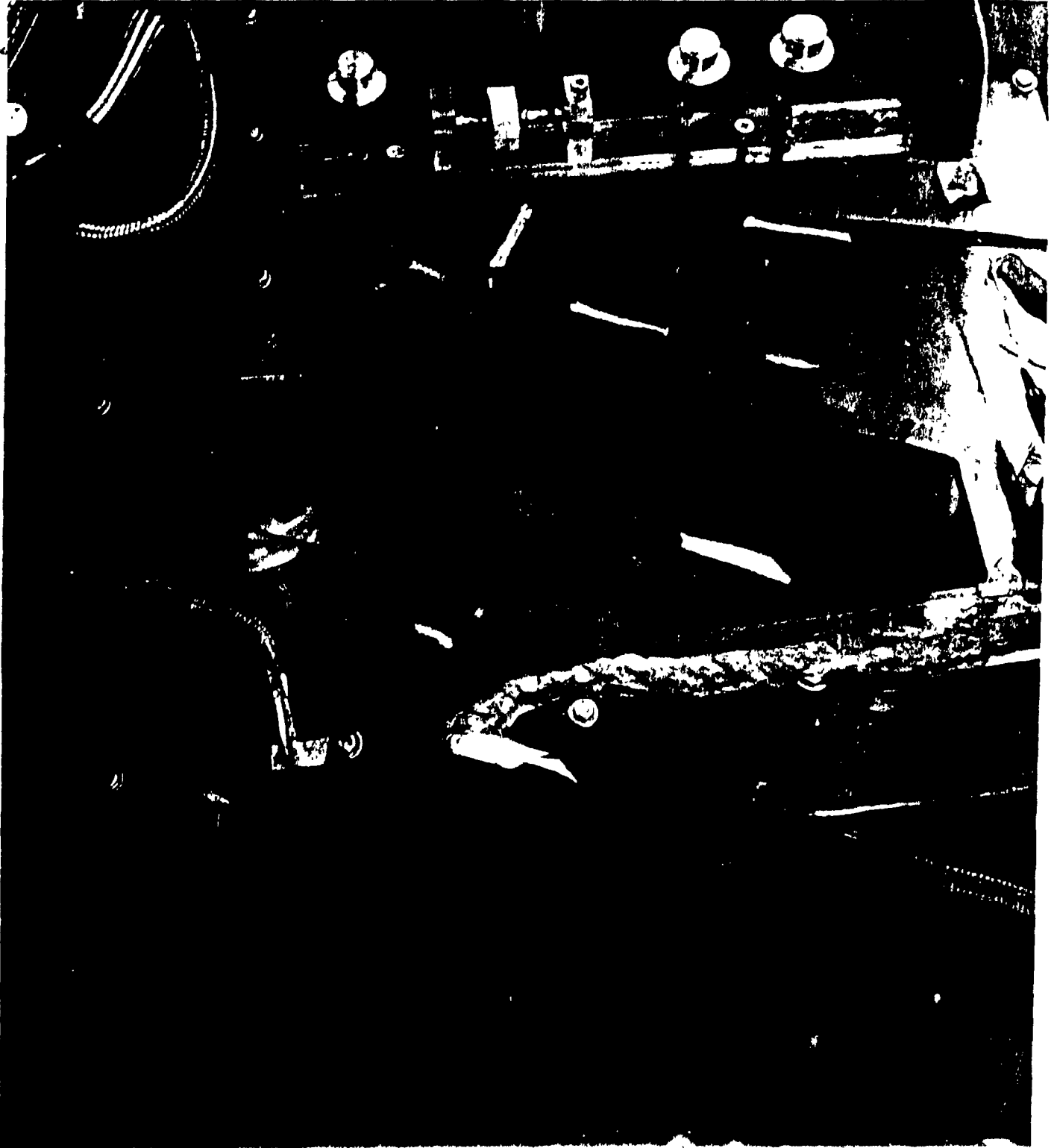


Fig. 10: CONTROL PANEL OF DYE INJECTOR.

Fig. 11: PASSAGE VORTEX INSIDE BLADE CHANNEL
AT ZERO CLEARANCE THROUGH VIEWING
PLANES 2, 3, 4.

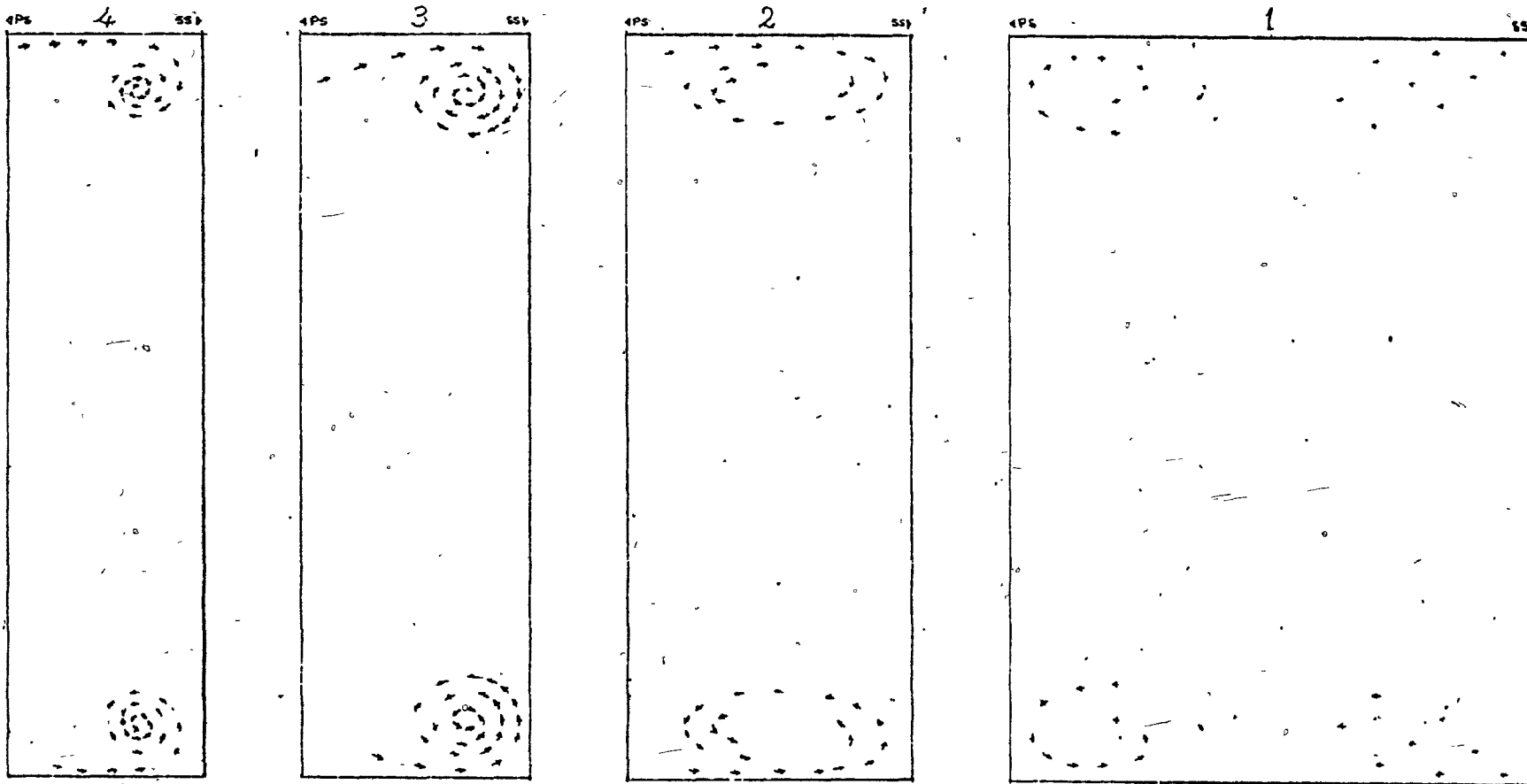
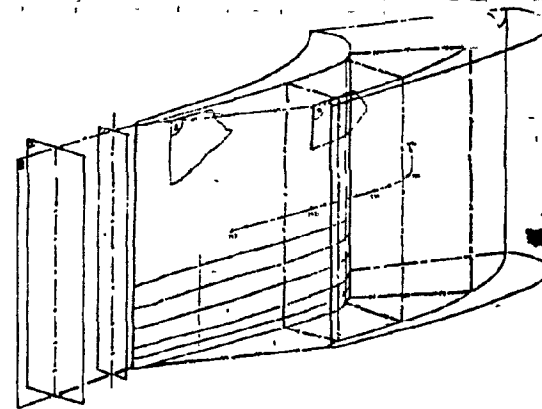
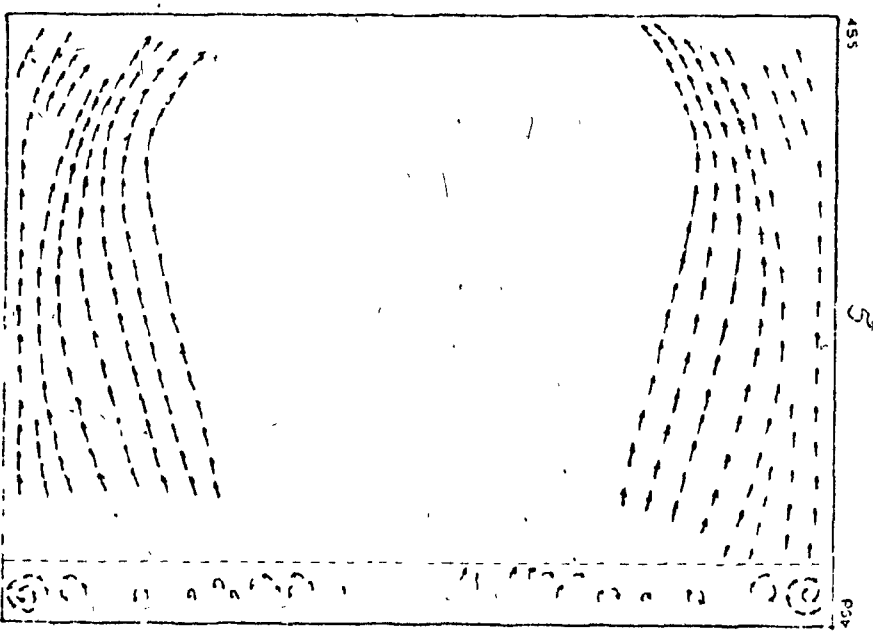
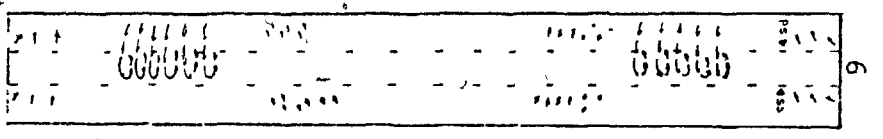
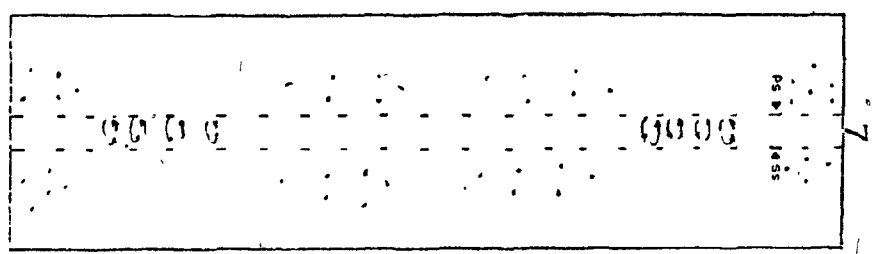
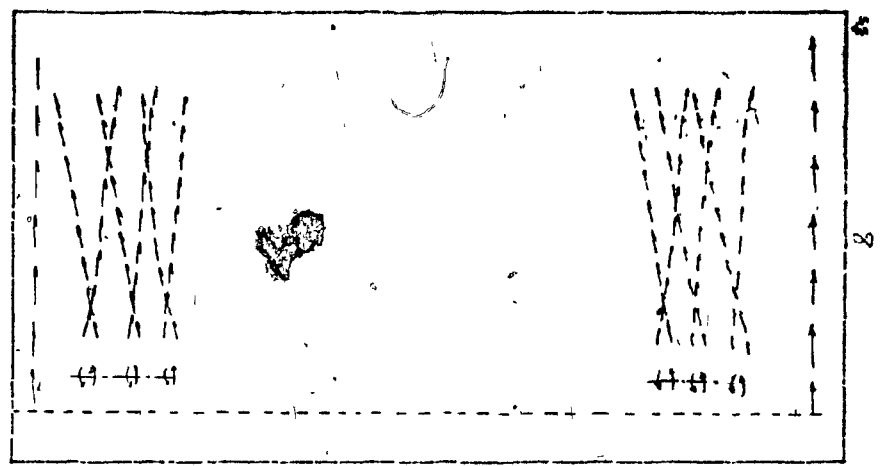
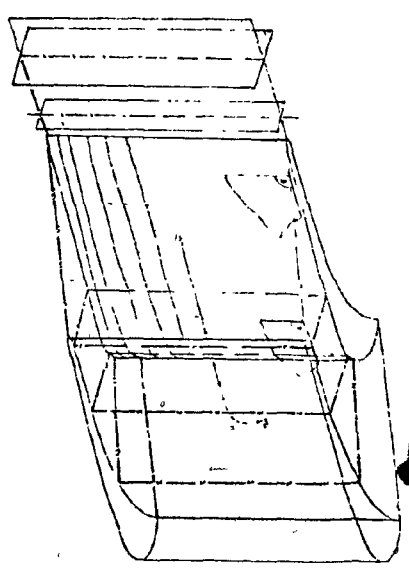


FIG. 12: EVIDENCES OF PASSAGE VORTEX AT VIEWING
 PLANE NO. 5, FORMATION OF TRAILING VORTICES
 DOWNSTREAM FROM TRAILING EDGE.



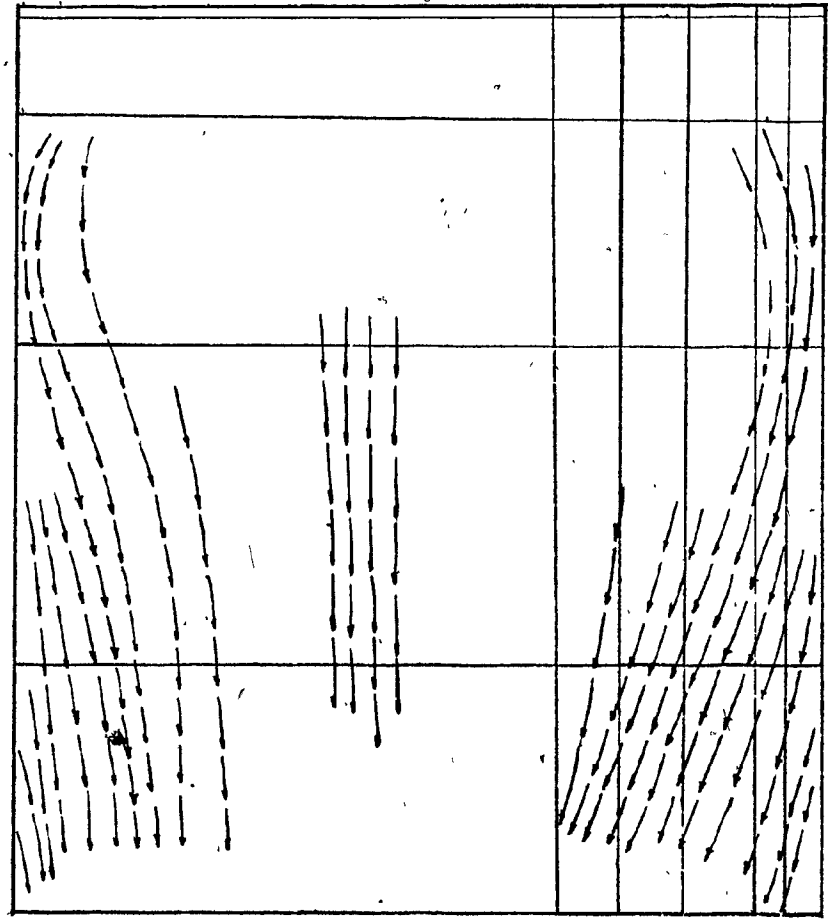
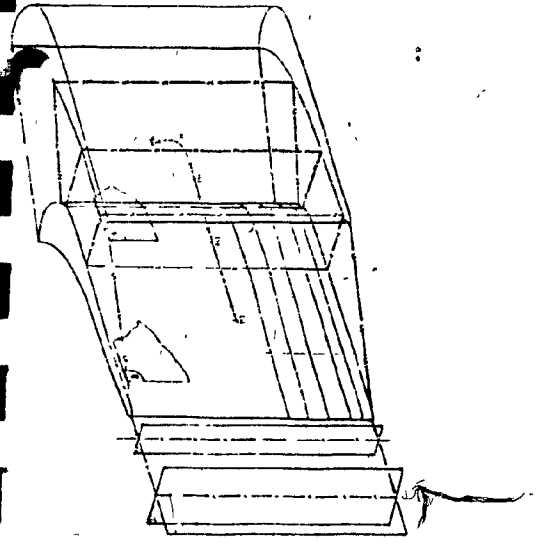


FIG. 13: SUCTION SURFACE FLOW DISTRIBUTION
AT ZERO CLEARANCE.

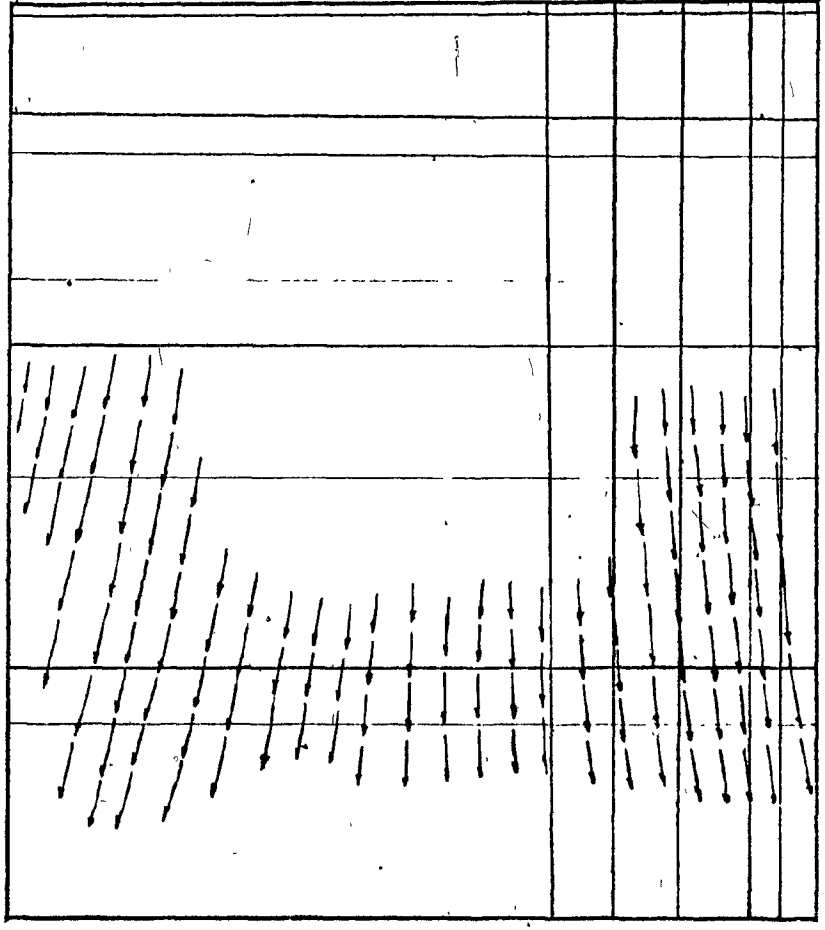
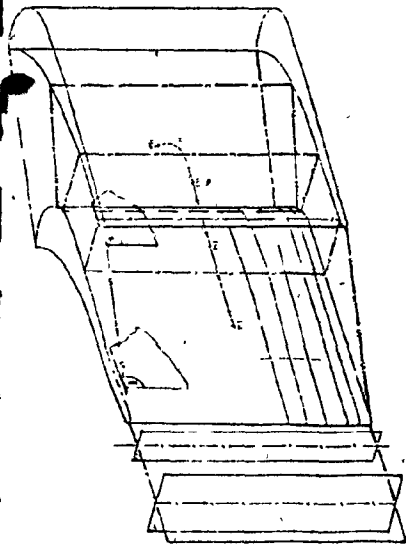
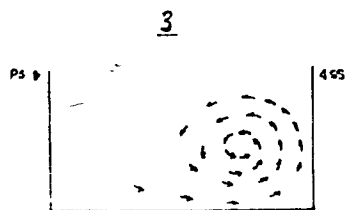
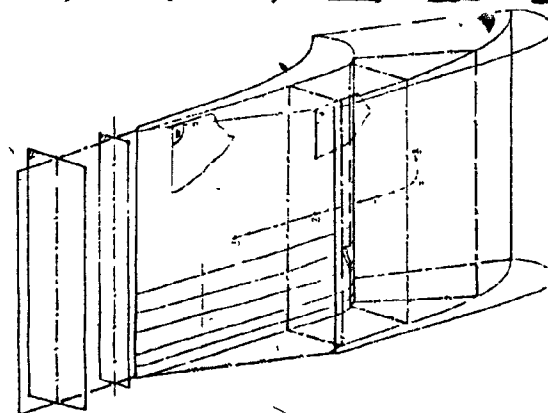
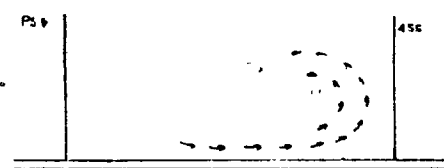
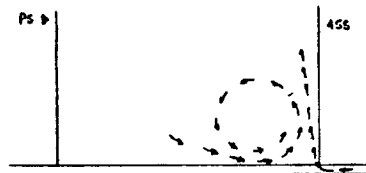
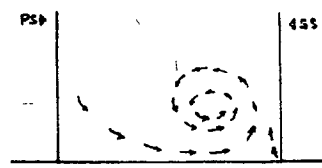


Fig. 14: PRESSURE SURFACE FLOW DISTRIBUTION
AT ZERO CLEARANCE.

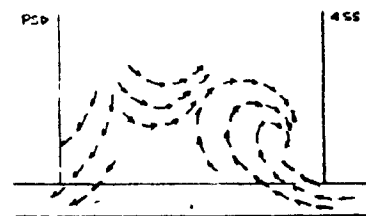
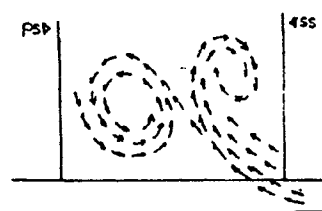
Fig. 15: EFFECT OF VARIATION OF TIP CLEARANCE.



15 a, ZERO TIP CLEARANCE



15 b, 0.5% TIP CLEARANCE



15 c, 2% TIP CLEARANCE

Fig. 16: EFFECT OF TIP CLEARANCE VORTEX ON TRAILING VORTICES AT 2% TIP CLEARANCE AND STATIONARY SMOOTH BELT CONDITION.

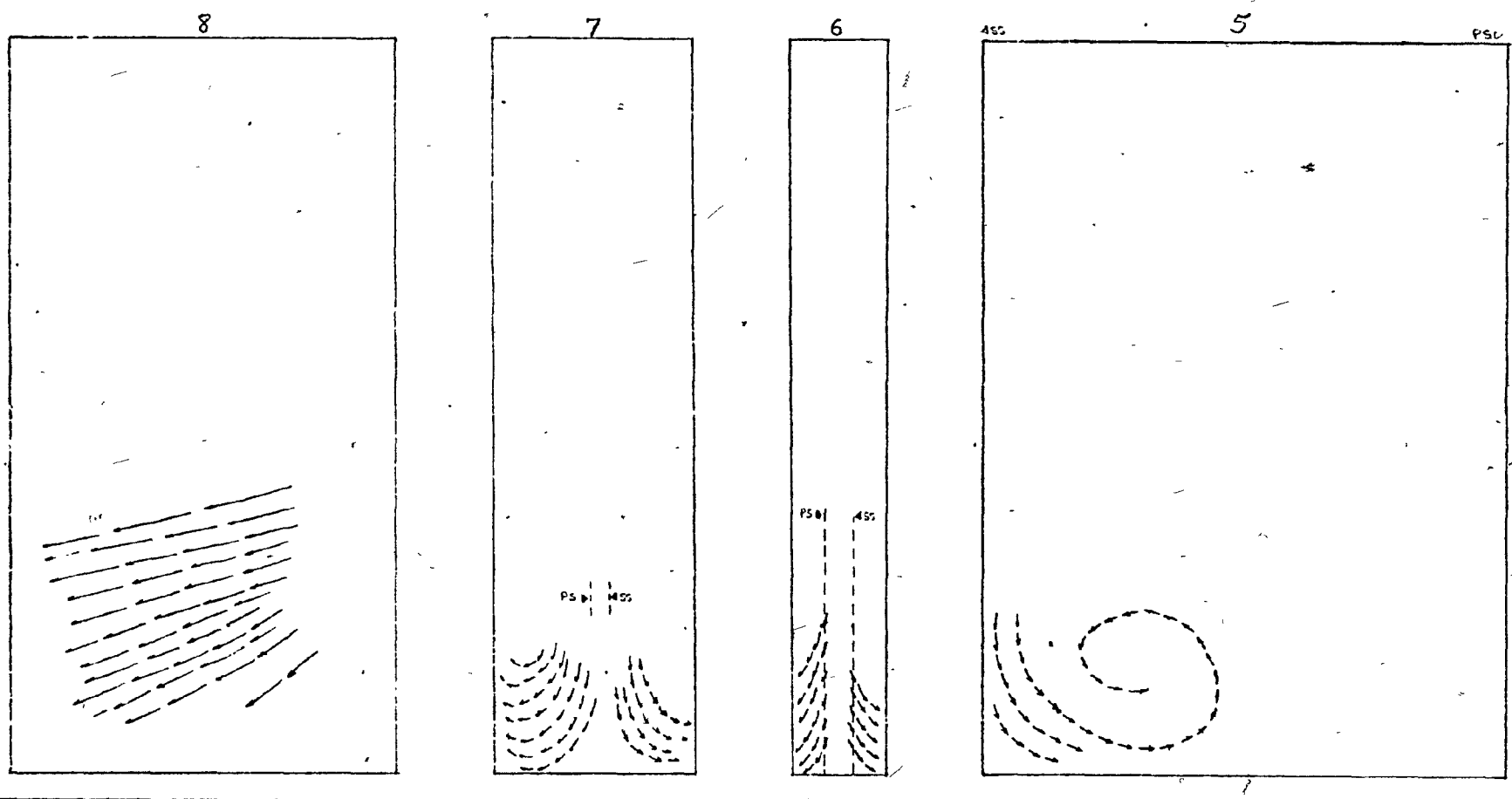
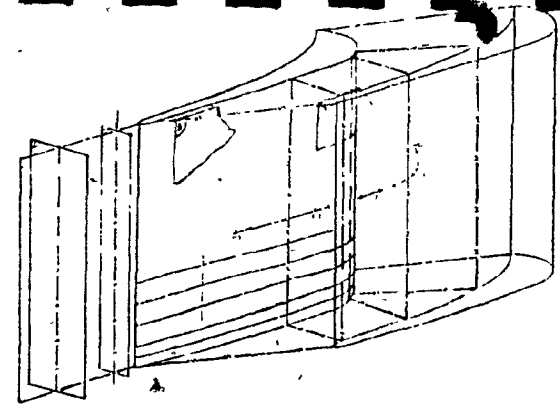
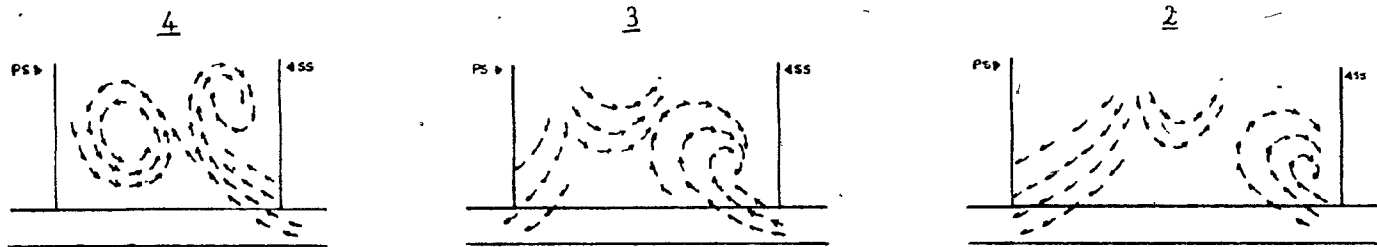
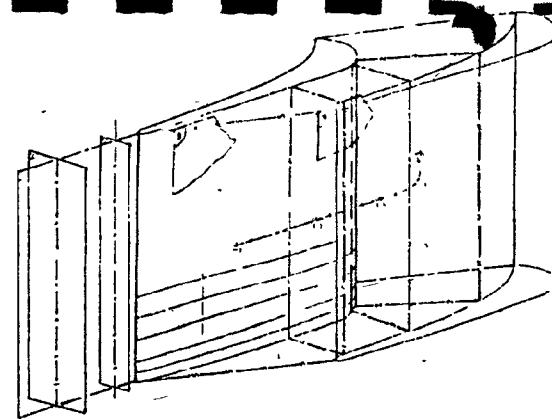
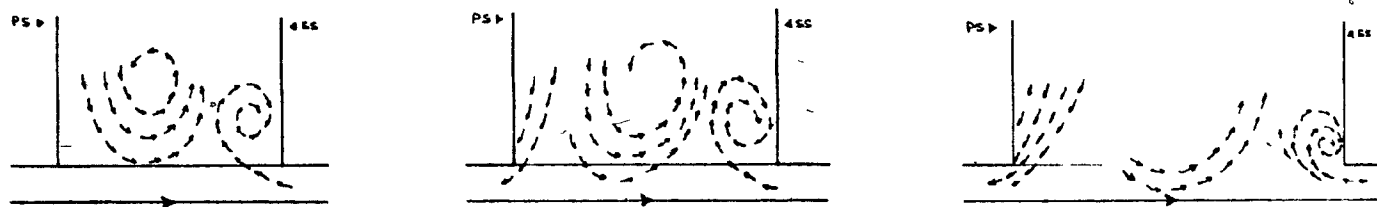


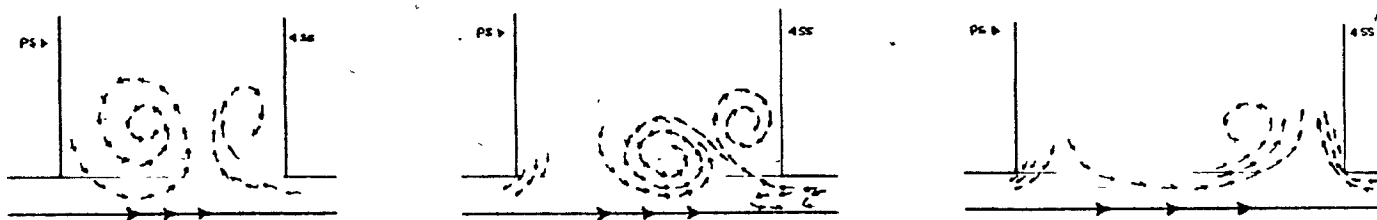
Fig. 17: EFFECT OF SPEED VARIATION.



17 a, 2% TIP CLEARANCE AT ZERO SPEED



17 b, 2% TIP CLEARANCE AT DESIGN POINT SPEED



17 c, 2% TIP CLEARANCE AT TRIPLE SPEED OF DESIGN POINT.

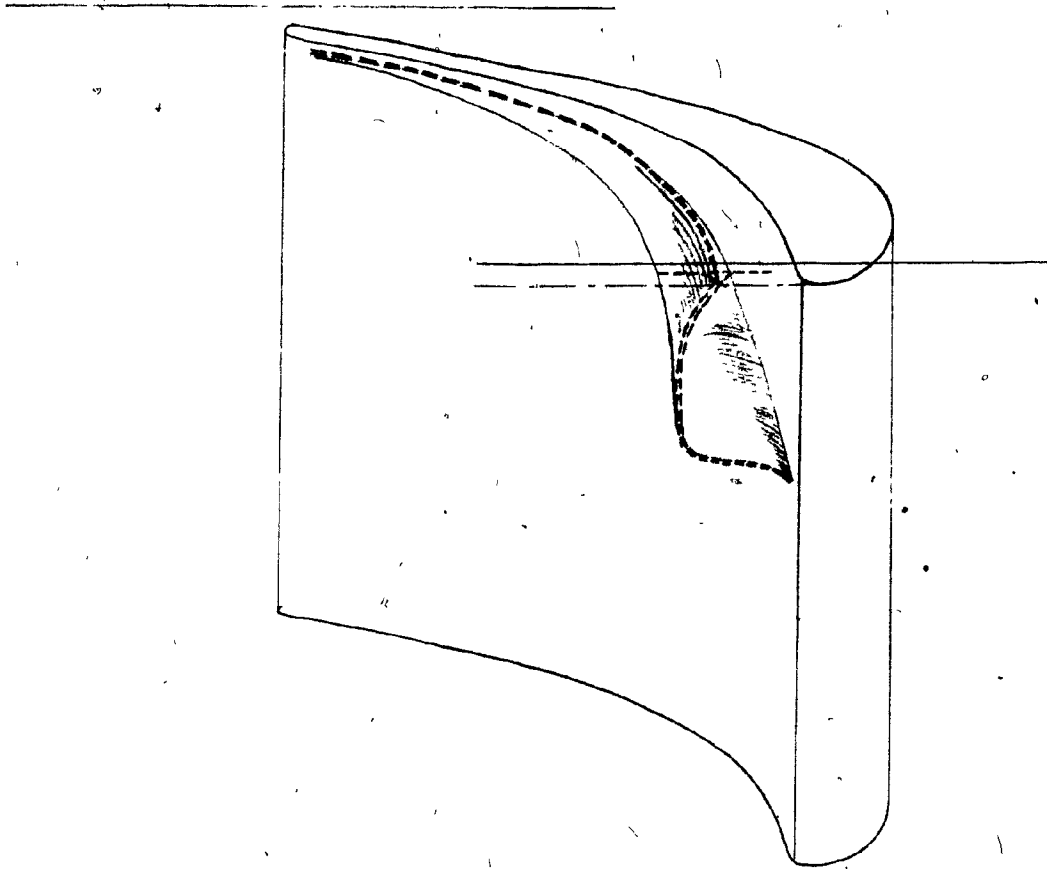


Fig. 18: DEFINITION OF LEAKAGE LINE
CRITERION.

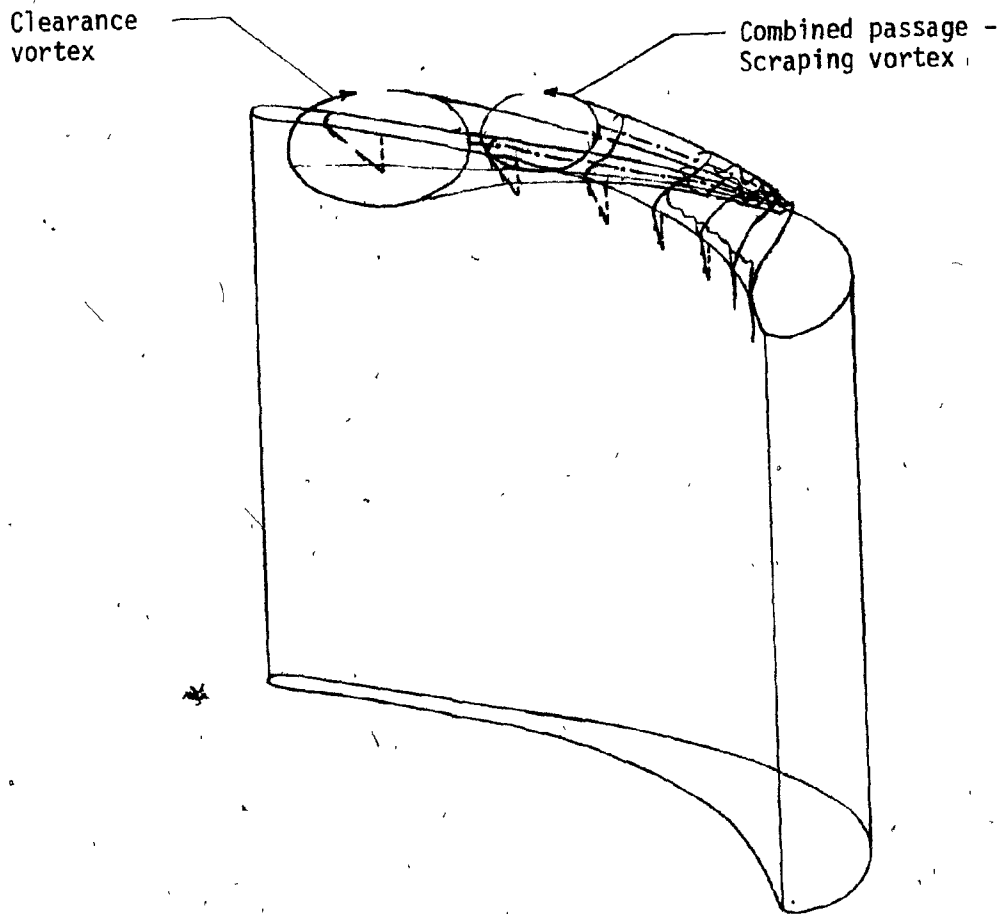


Fig. 19: DEFINITION OF PRESSURE SURFACE STREAMLINE
DIRECTION, TIP LEAKAGE FLOW DIRECTION, AND
SECONDARY VORTICES BOUNDARY CRITERIA.

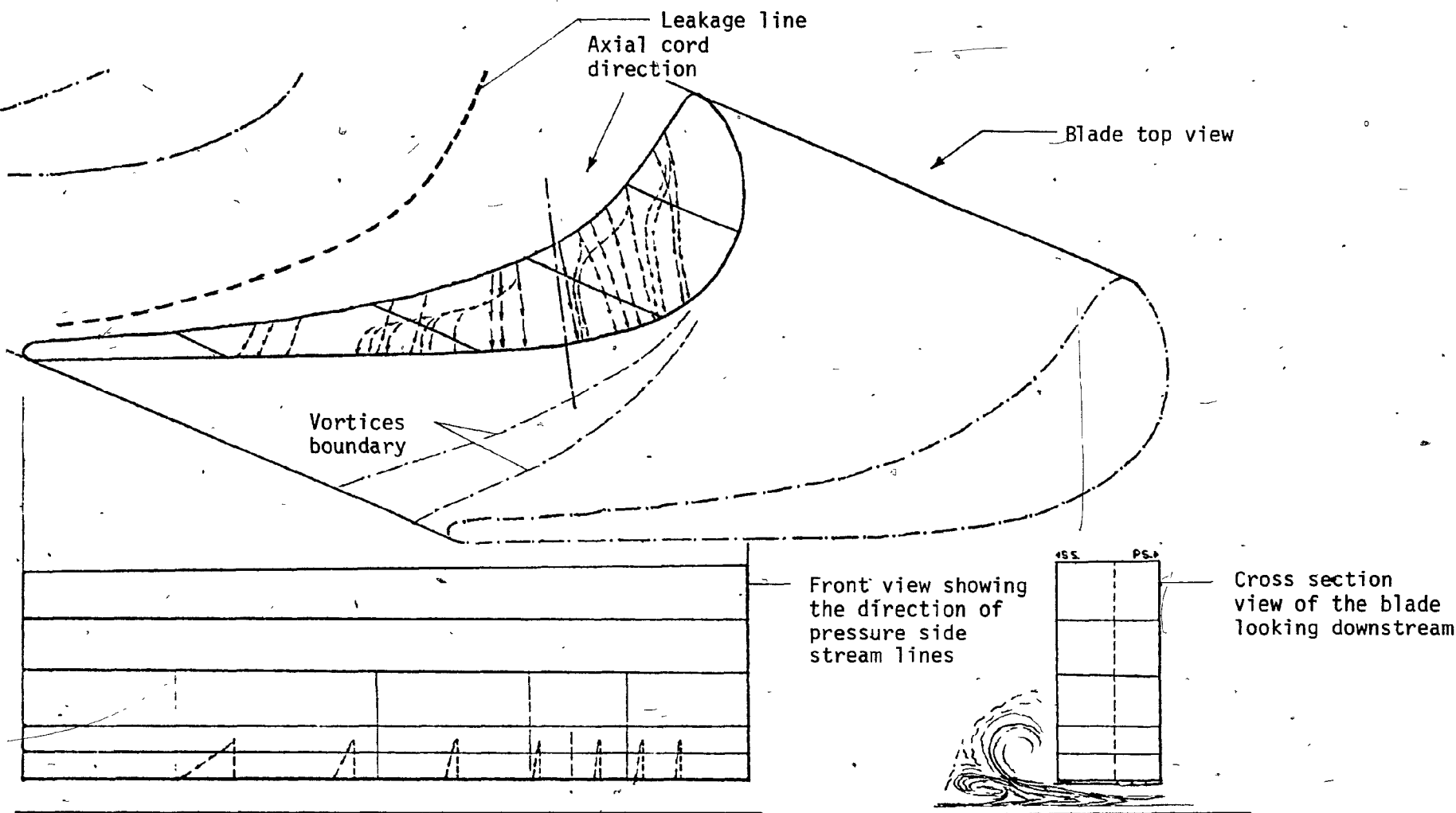
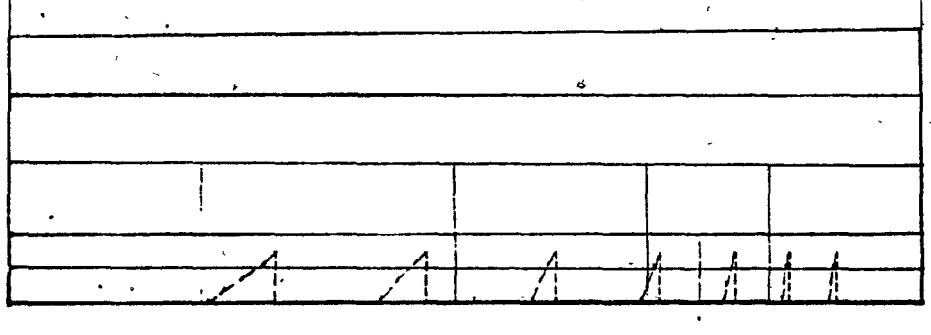
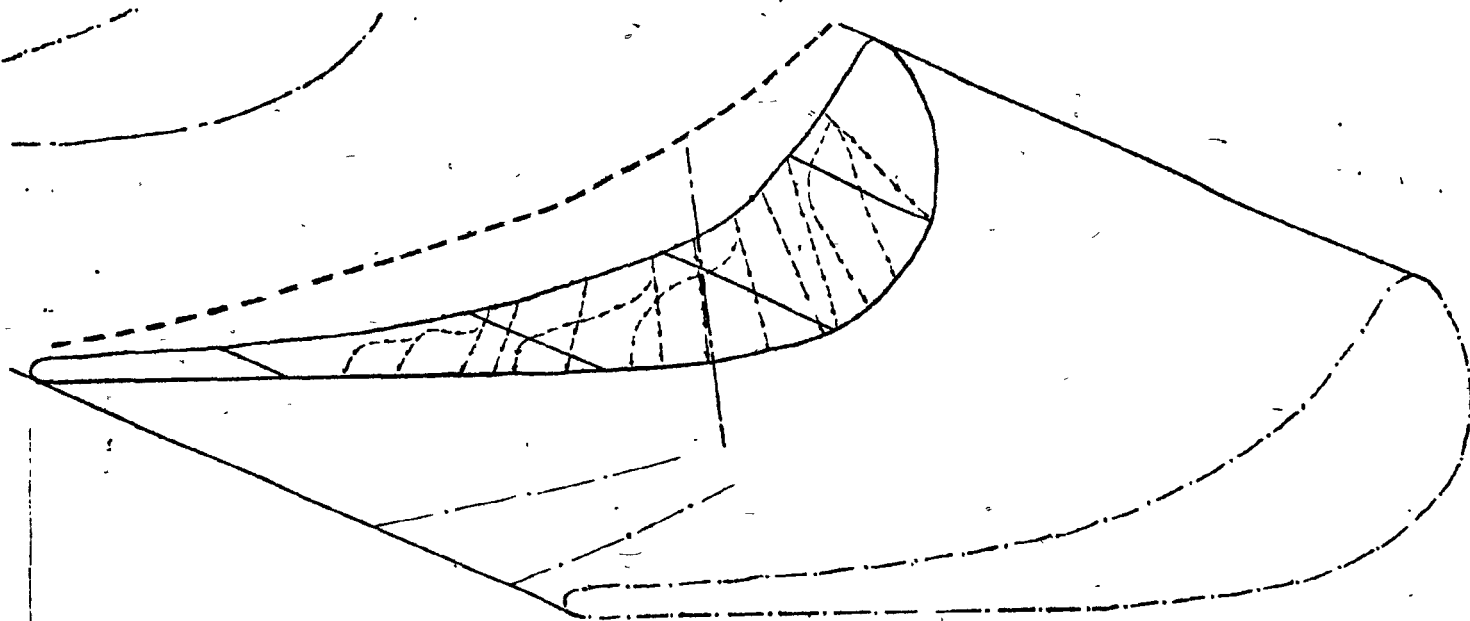


Fig. 20: OBSERVATION RESULTS FOR 2.5% TIP CLEARANCE
 WITH SMOOTH BELT RUNNING AT THE DESIGN
 POINT EQUIVALENT SPEED.



455	PS.6



Fig. 21: OBSERVATION RESULTS FOR 2% TIP CLEARANCE
 WITH SMOOTH BELT RUNNING AT THE DESIGN
 POINT EQUIVALENT SPEED.

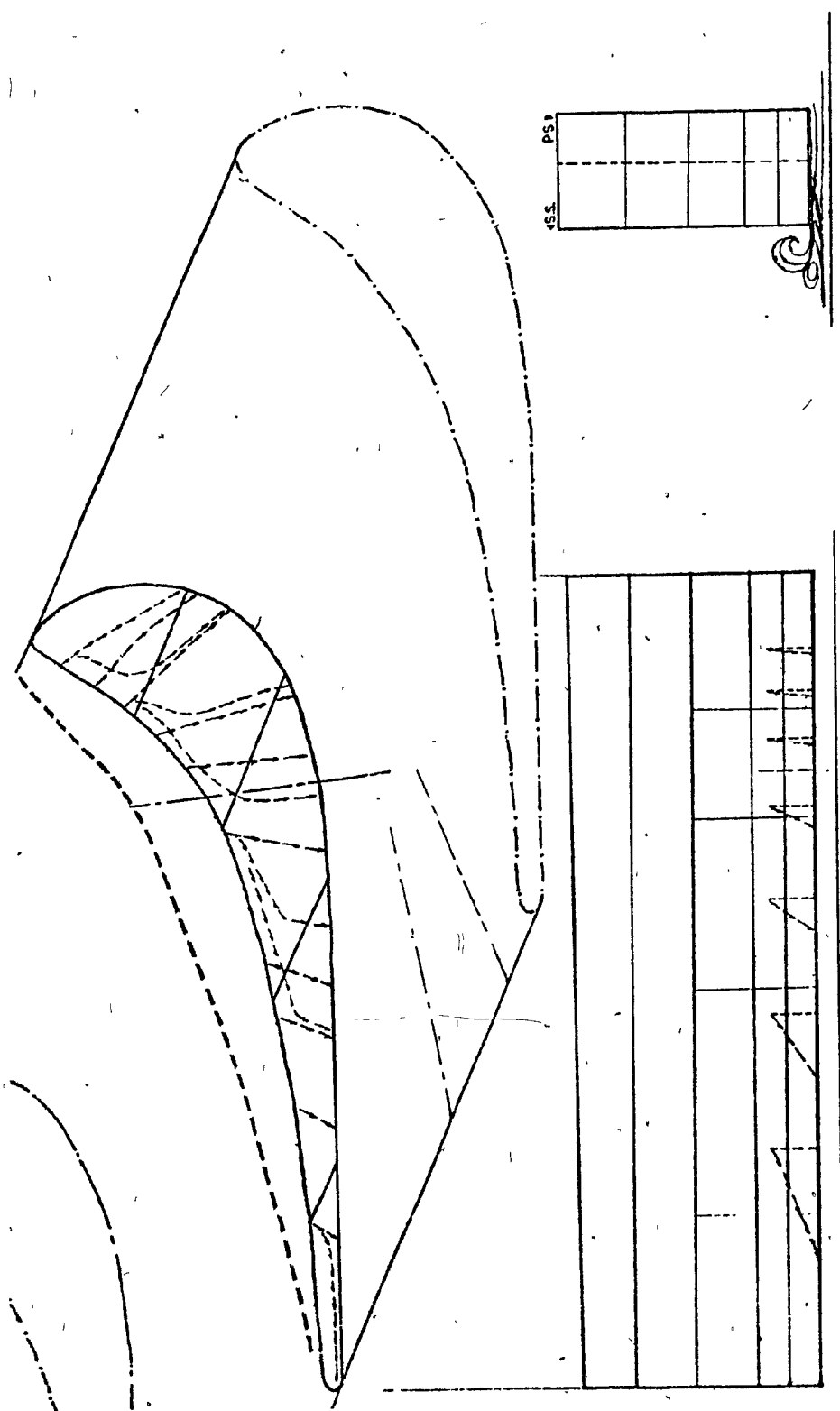


Fig. 22: OBSERVATION RESULTS FOR 1.5% TIP CLEARANCE
WITH SMOOTH BELT RUNNING AT THE DESIGN
POINT EQUIVALENT SPEED.

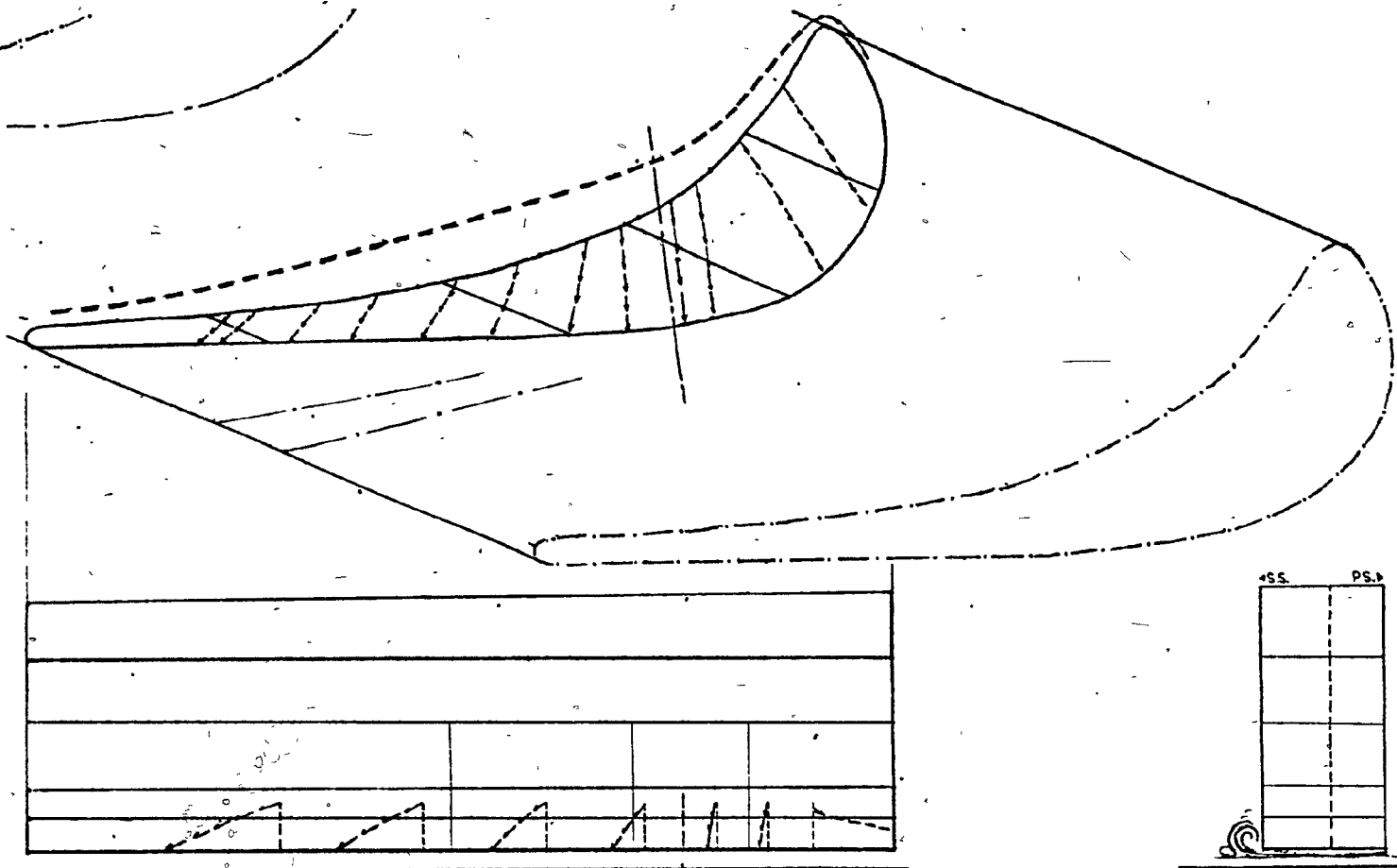
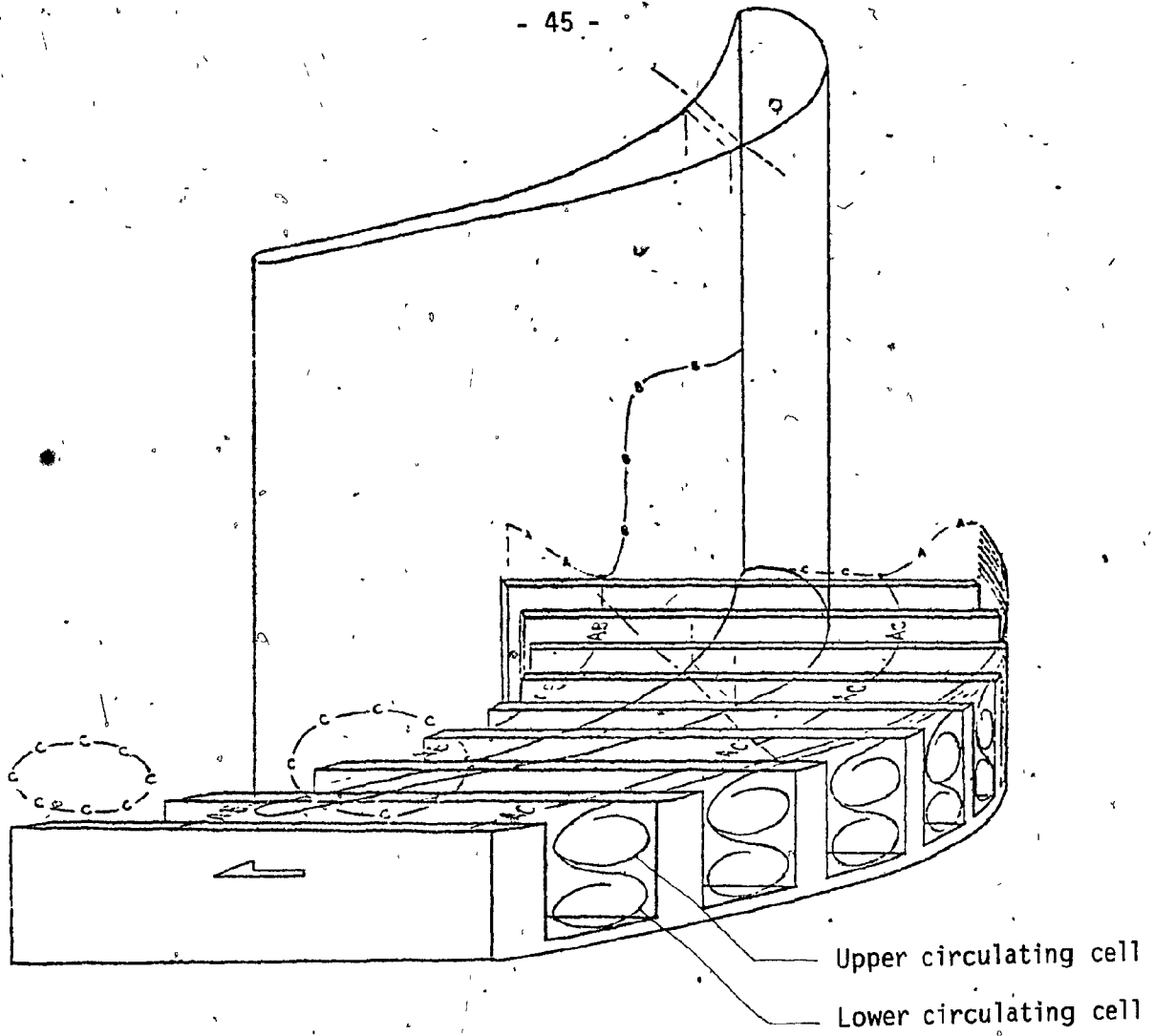


Fig. 23: OBSERVATION RESULTS FOR 1% TIP CLEARANCE
 WITH SMOOTH BELT RUNNING AT THE DESIGN
 POINT EQUIVALENT SPEED.



Peak outflow corresponds to the blade suction side

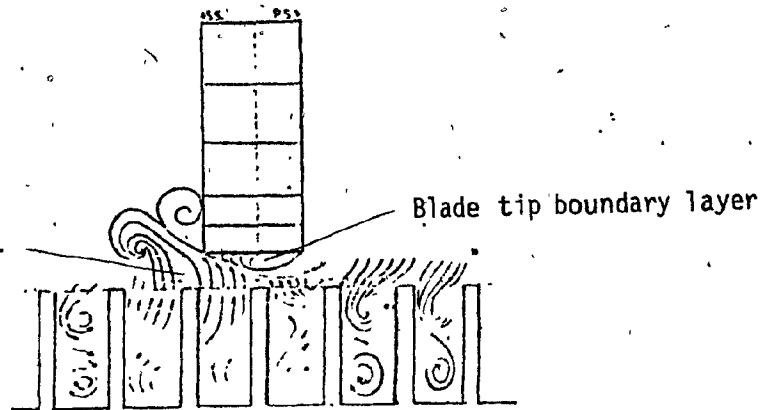


Fig. 24: FLOW MECHANISM INSIDE THE GROOVES.



Fig. 25: FLOW MECHANISM ALONG THE GROOVES.

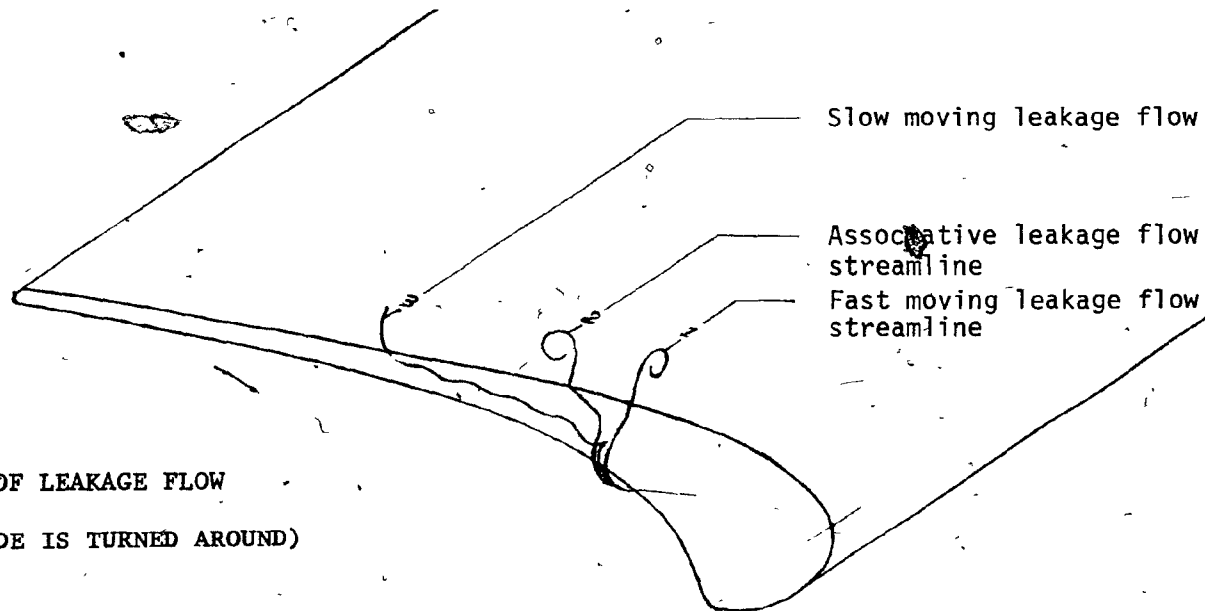
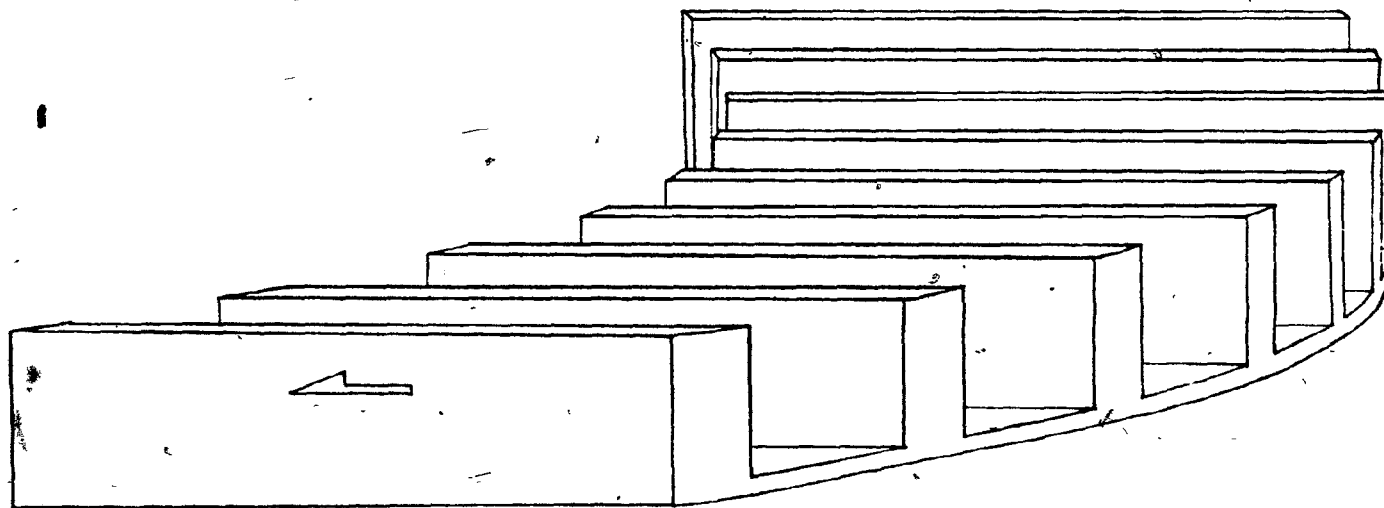


Fig. 26:- THREE DIFFERENT TYPES OF LEAKAGE FLOW PATTERNS. (BLADE CASCADE IS TURNED AROUND)



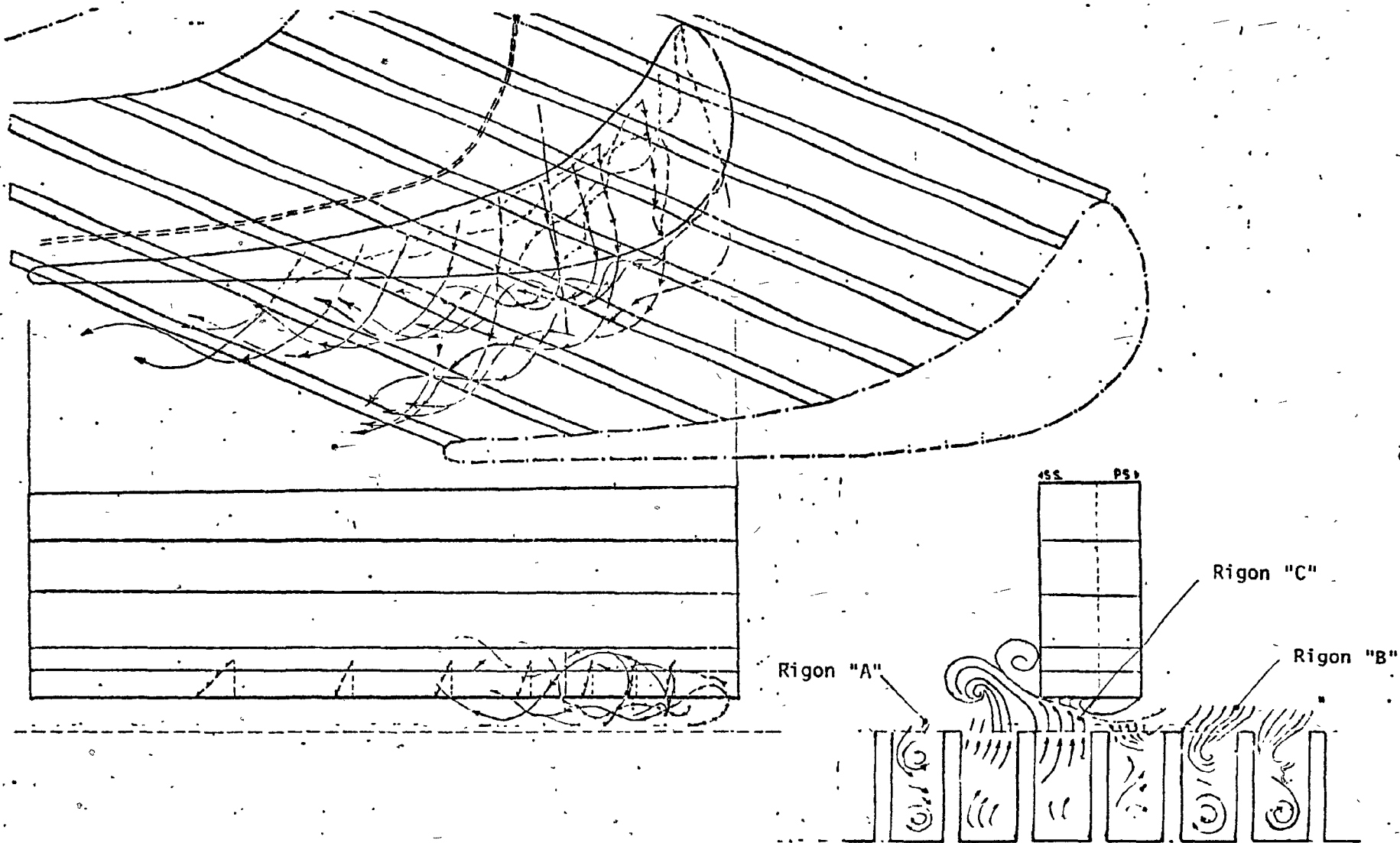


Fig. 27: OBSERVATION RESULTS FOR 2.5% TIP CLEARANCE
IN STATIONARY GROOVED BELT CONDITION.

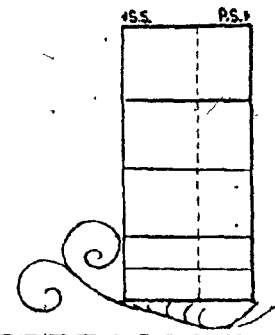
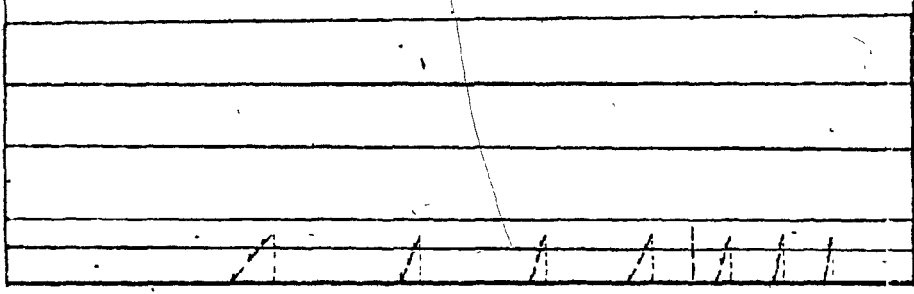
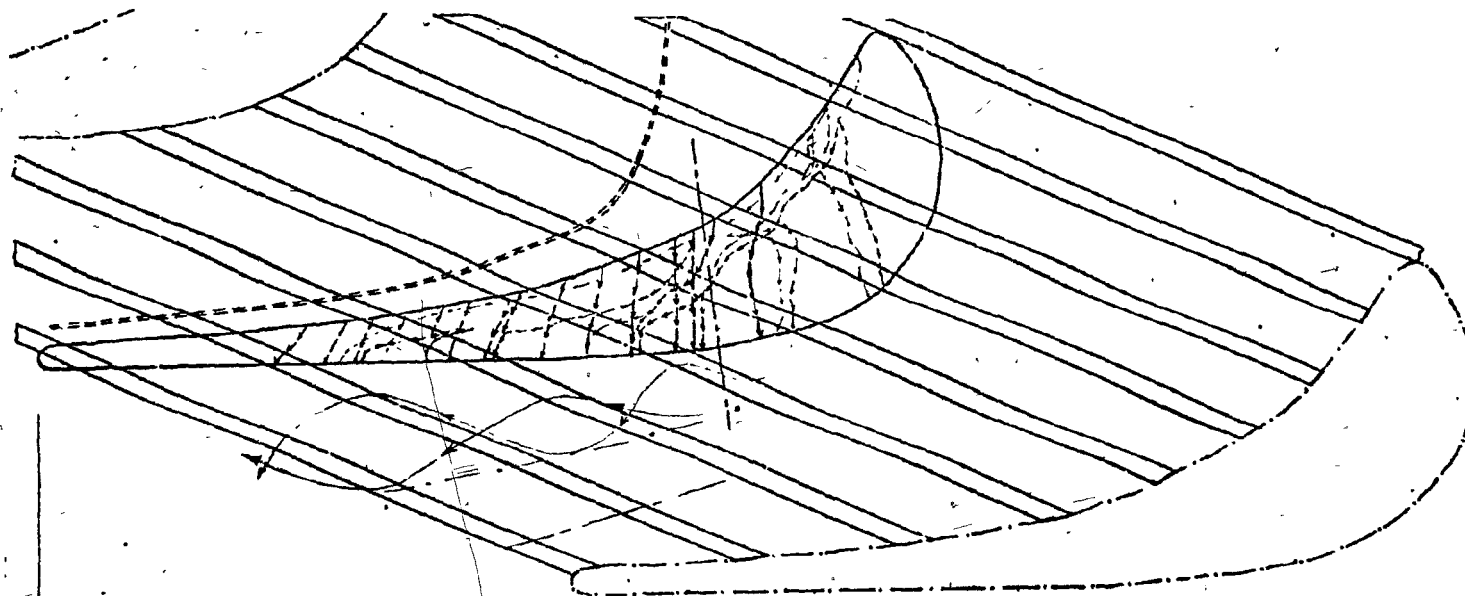
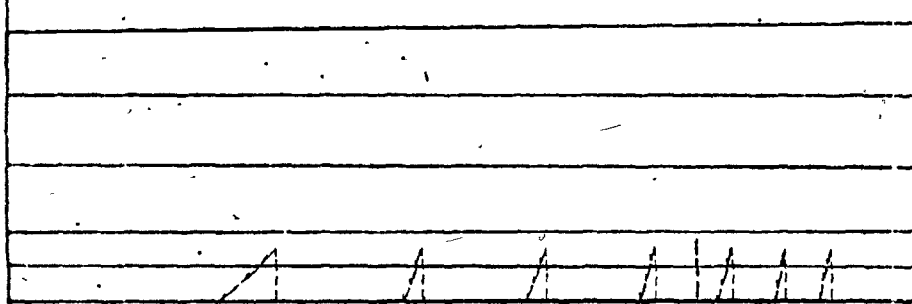
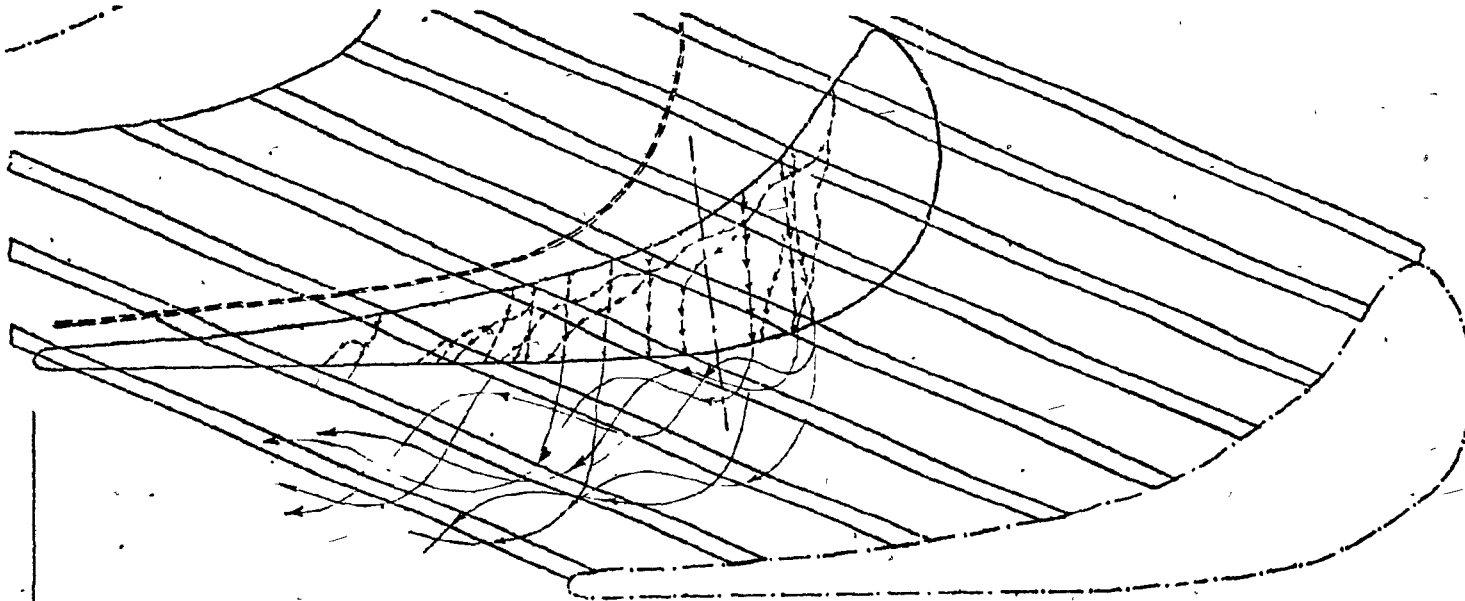


Fig. 28: OBSERVATION RESULTS FOR 2% TIP CLEARANCE
 IN STATIONARY GROOVED BELT CONDITION.



SS	PS

Fig. 29: OBSERVATION RESULTS FOR 1.5% TIP CLEARANCE
IN STATIONARY GROOVED BELT CONDITION.

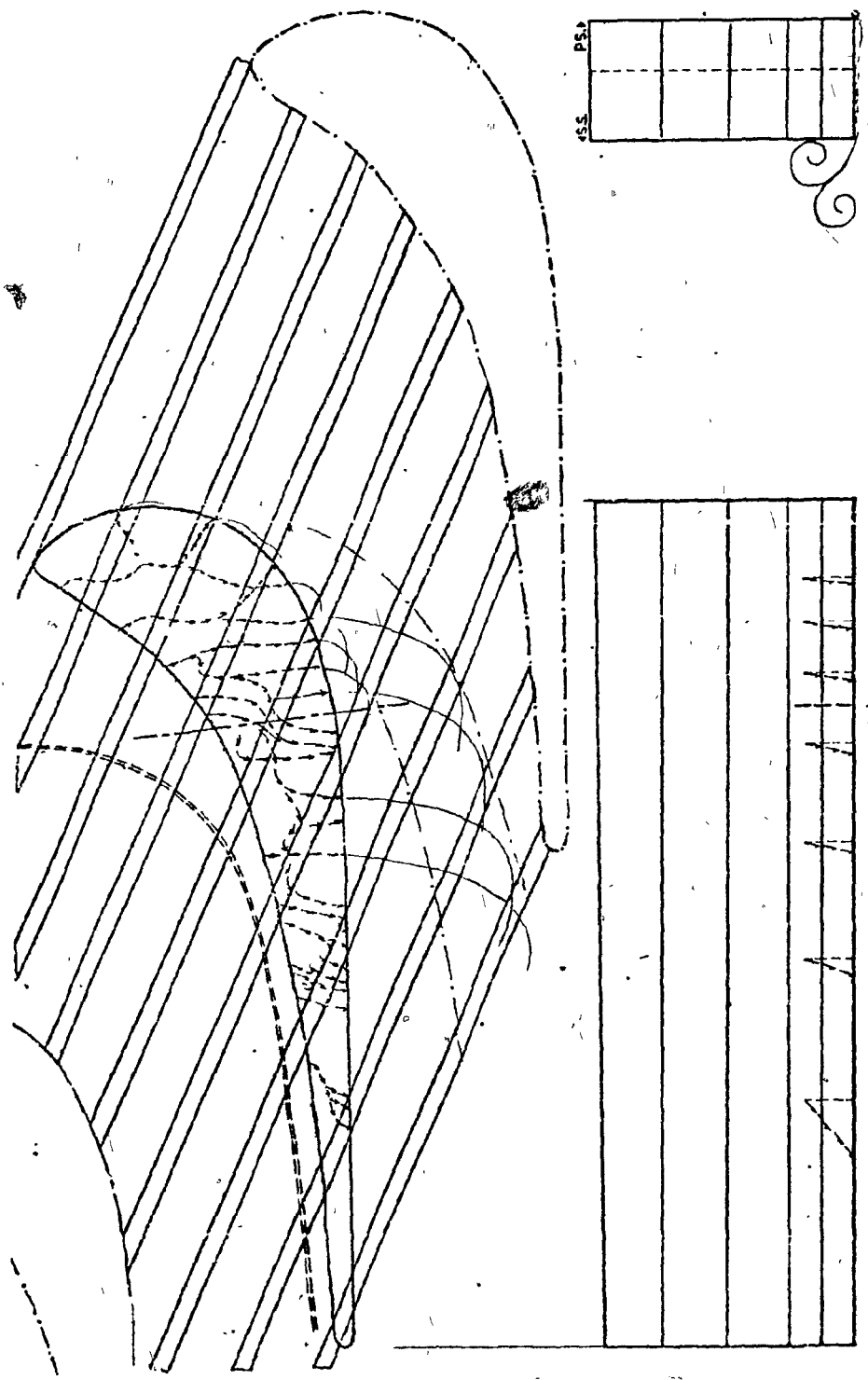


Fig. 30: OBSERVATION RESULTS FOR 1% TIP CLEARANCE
IN STATIONARY GROOVED BELT CONDITION.

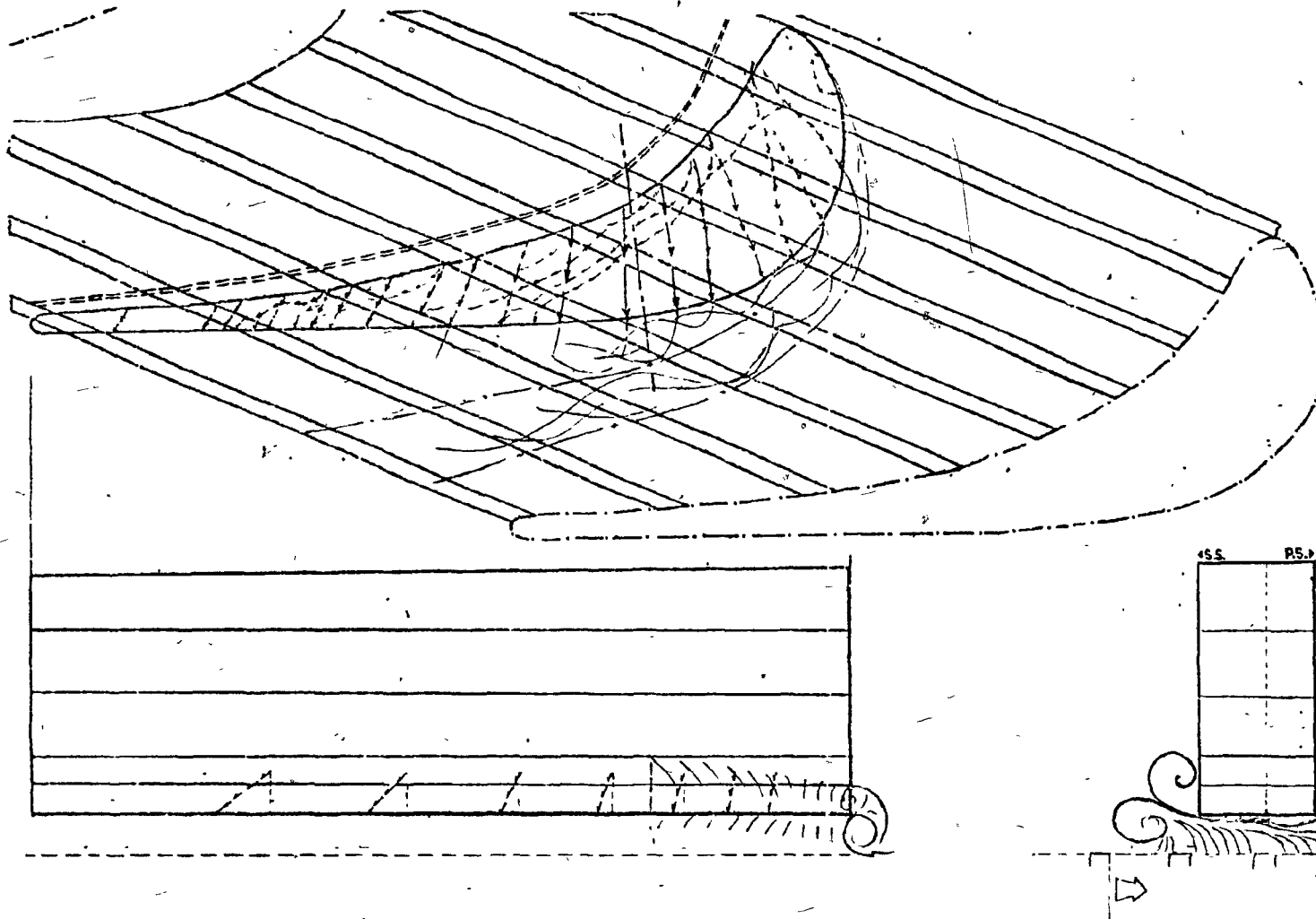


Fig. 31: OBSERVATION RESULTS FOR 2.5% TIP CLEARANCE,
 WITH THE GROOVED BELT RUNNING AT THE DESIGN
 POINT EQUIVALENT SPEED.

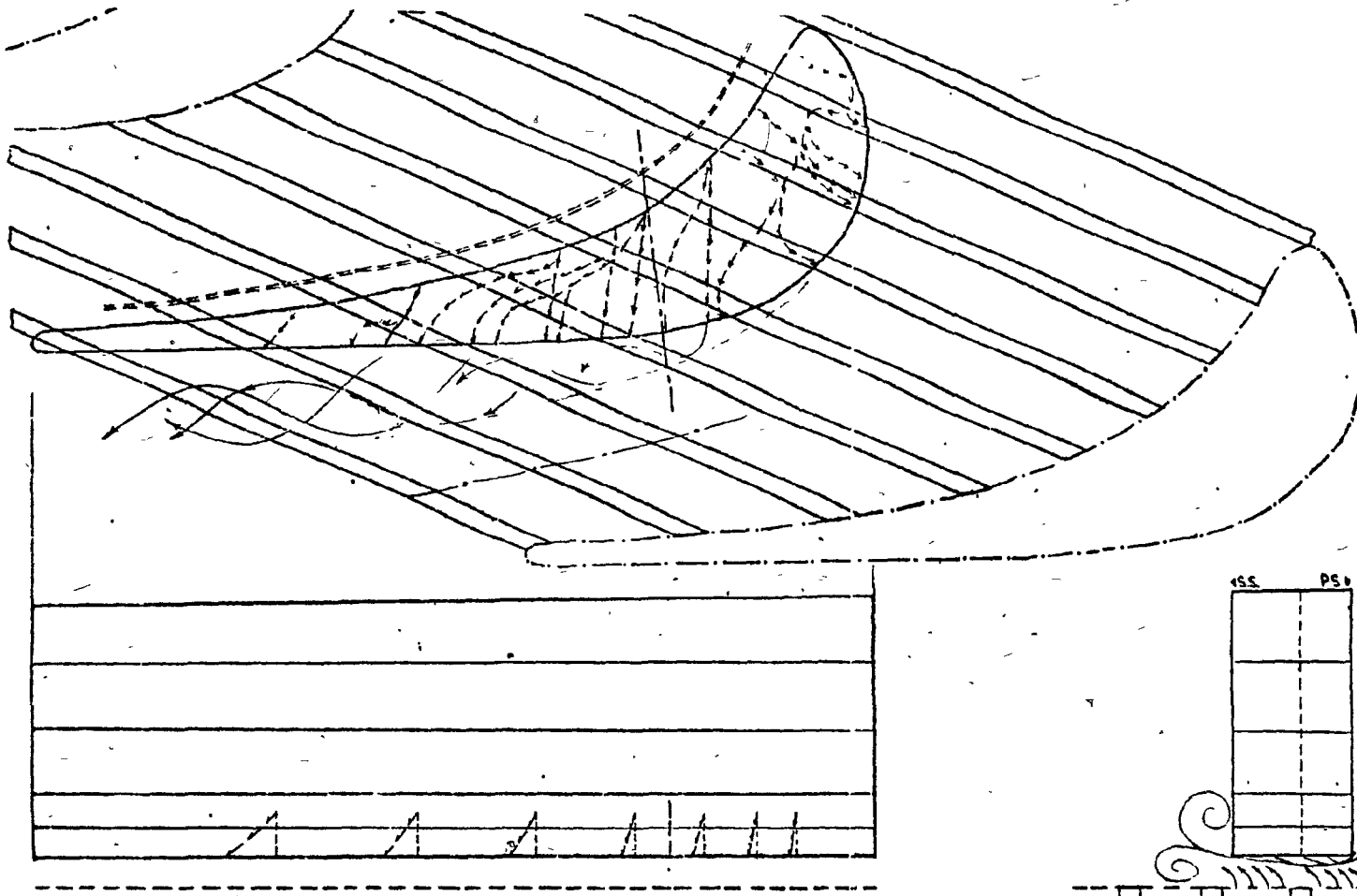
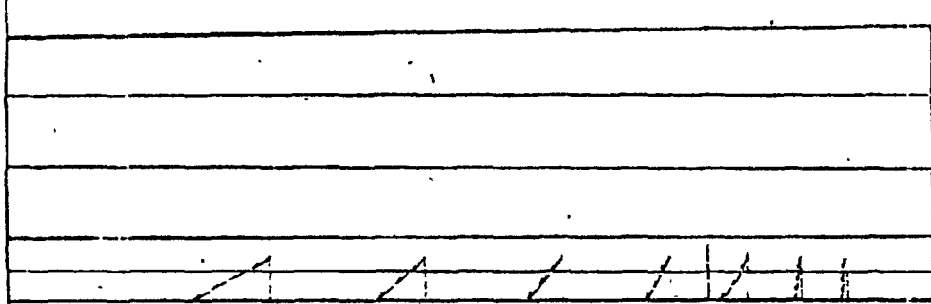
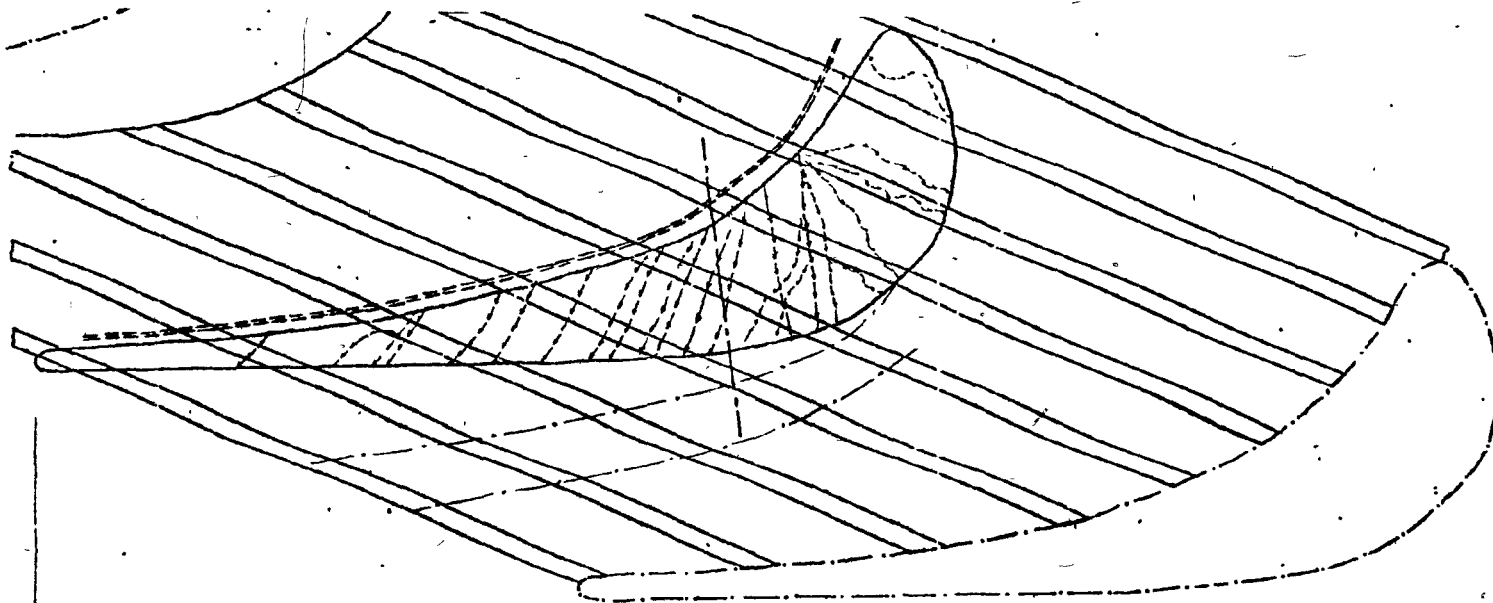


Fig. 32: OBSERVATION RESULTS FOR 2% TIP CLEARANCE,
 WITH THE GROOVED BELT RUNNING AT THE DESIGN
 POINT EQUIVALENT SPEED.



SS	PS

Fig. 33: OBSERVATION RESULTS FOR 1.5% TIP CLEARANCE,
 WITH THE GROOVED BELT RUNNING AT THE DESIGN
 POINT EQUIVALENT SPEED.

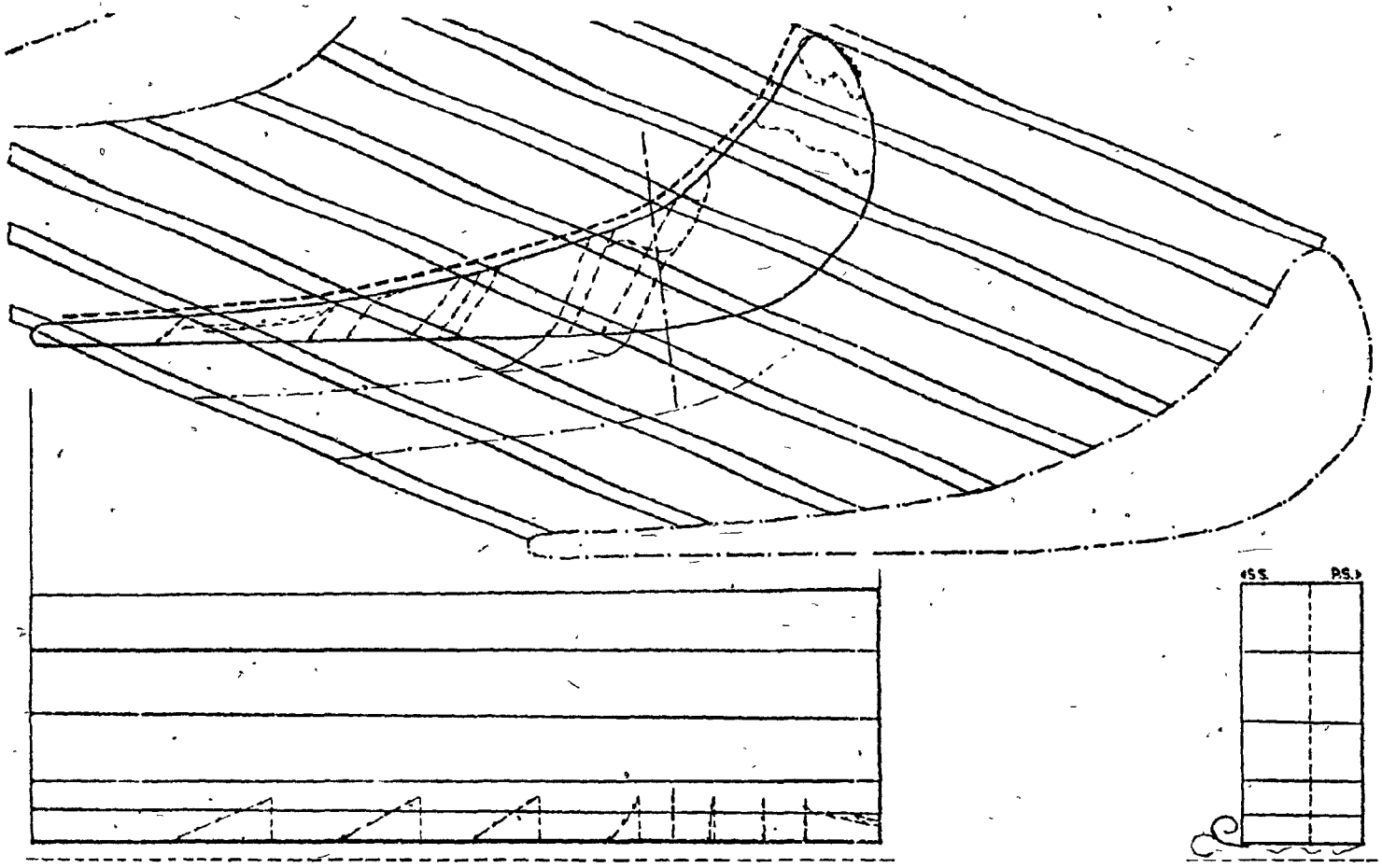
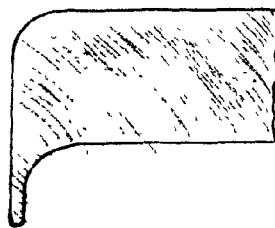
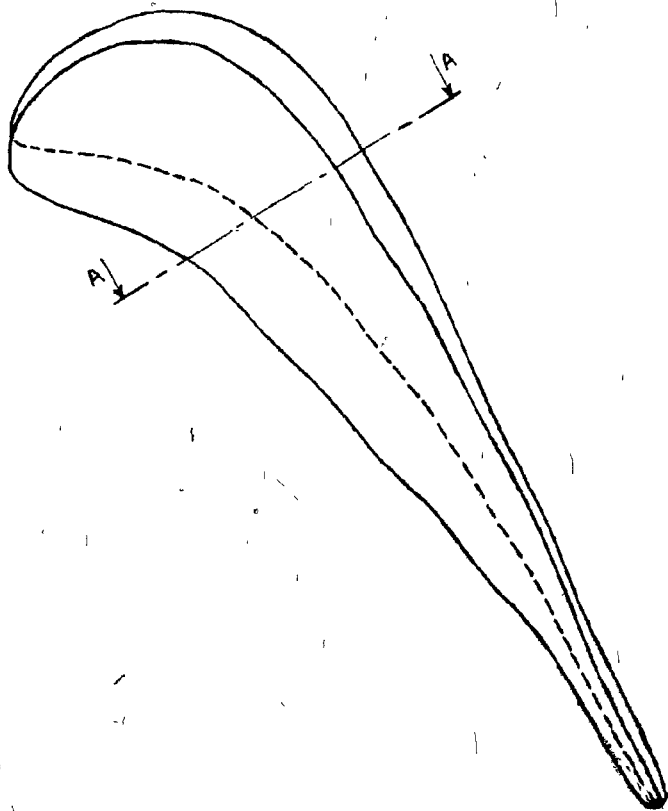
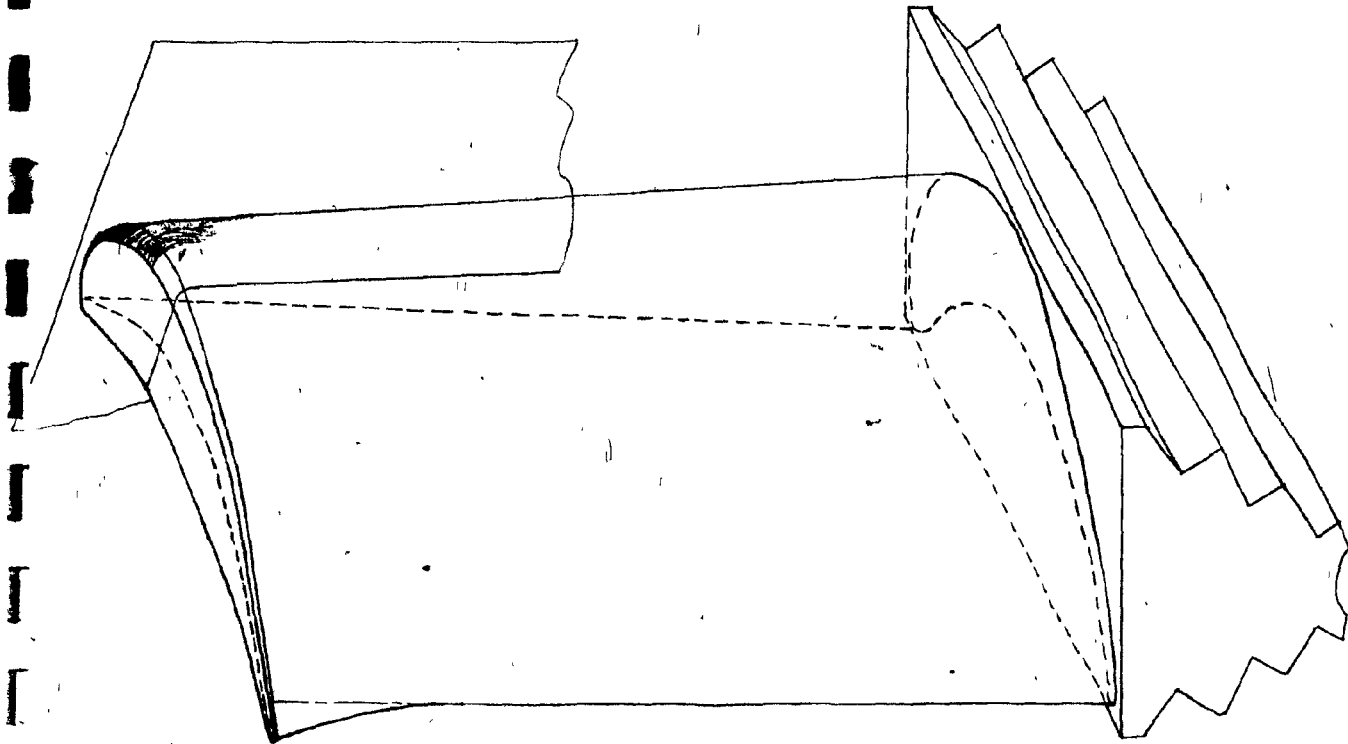


Fig. 34: OBSERVATION RESULTS FOR 1% TIP CLEARANCE,
 WITH THE GROOVED BELT RUNNING AT THE DESIGN
 POINT EQUIVALENT SPEED.

5



Cross section A.A

Fig. 35: RECOMMENDED BLADE TIP CONFIGURATION
FOR REDUCTION OF THE LEAKAGE FLOW.

11. APPENDIX

Secondary Flows

Secondary flows that are responsible for approximately 4.4% of the turbine efficiency drop (Ref. 3) may be classified as follows:

1) The passage vortex:

Cross flows in the blade channel due to turning the flow. Under the influence of the passage vortex fluid adjacent to the end walls travels from the pressure side to the suction side.

2) The scraping vortex:

Cross flows in the blade channel due to the collision of the blade tip leakage flow boundary layer and the casing wall boundary layer develop the scraping vortex. This collision scrapes up the casing wall boundary layer and forms a vortex that rotates in the same direction as the passage vortex. At the blade tip region the scraping vortex joins the passage vortex and forms the "combined passage-scraping vortex"* (Fig. 3).

3) The clearance vortex

Leakage flows through the tip clearance, develops the clearance vortex that rolls up in the blade suction side corner. The direction of the clearance vortex is in the opposite direction to the combined passage-scraping vortex (Fig. 3).

* For the circumferentially grooved casing wall, a groove outflow vortex exists in the place of the scraping vortex, and at the blade tip region this groove outflow vortex joins the passage vortex and forms the "combined passage-groove outflow vortex".

4) Trailing vortex

Trailing vortices are caused by the difference between the flow distribution in the pressure side and the suction side of the blade.

5) Von Karman eddies

Von Karman eddies form in the wake region, downstream from the trailing edge. These eddies rotate around an axis perpendicular to the turbine axis.